Published for SISSA by Springer

Received: March 14, 2015
Revised: May 20, 2015
Accepted: June 2, 2015
Published: June 25, 2015

Scrutinizing the η-η' mixing, masses and pseudoscalar decay constants in the framework of U(3) chiral effective field theory

Xu-Kun Guo,[a] **Zhi-Hui Guo,**[a,b,1] **José Antonio Oller**[c] **and Juan José Sanz-Cillero**[d]

[a] *Department of Physics, Hebei Normal University, Shijiazhuang 050024, People's Republic of China*

[b] *State Key Laboratory of Theoretical Physics, Institute of Theoretical Physics, CAS, Beijing 100190, People's Republic of China*

[c] *Departamento de Física, Universidad de Murcia, E-30071 Murcia, Spain*

[d] *Departamento de Física Teórica and Instituto de Física Teórica, IFT-UAM/CSIC, Universidad Autónoma de Madrid, Cantoblanco, 28049 Madrid, Spain*

E-mail: 1042007825@qq.com, zhguo@mail.hebtu.edu.cn, oller@um.es, juanj.sanz@uam.es

Abstract: We study the η-η' mixing up to next-to-next-to-leading-order in U(3) chiral perturbation theory in the light of recent lattice simulations and phenomenological inputs. A general treatment for the η-η' mixing at higher orders, with the higher-derivative, kinematic and mass mixing terms, is addressed. The connections between the four mixing parameters in the two-mixing-angle scheme and the low energy constants in the U(3) chiral effective theory are provided both for the singlet-octet and the quark-flavor bases. The axial-vector decay constants of pion and kaon are studied in the same order and confronted with the lattice simulation data as well. The quark-mass dependences of m_η, $m_{\eta'}$ and m_K are found to be well described at next-to-leading order. Nonetheless, in order to simultaneously describe the lattice data and phenomenological determinations for the properties of light pseudoscalars π, K, η and η', the next-to-next-to-leading order study is essential. Furthermore, the lattice and phenomenological inputs are well reproduced for reasonable values of low the energy constants, compatible with previous bibliography.

Keywords: Effective field theories, Chiral Lagrangians

ArXiv ePrint: 1503.02248

[1] Corresponding author.

Open Access, © The Authors.
Article funded by SCOAP[3].

doi:10.1007/JHEP06(2015)175

Contents

JHEP06(2015)175

1 Introduction

The phenomenology of light flavor pseudoscalar mesons η and η' provides a valuable window on many important nonperturbative features of Quantum Chromodynamics (QCD). It includes such important aspects as:

- The spontaneous breaking of chiral symmetry, which gives rise to the appearance of the multiplet of light pseudoscalar mesons.
- The $\mathrm{U}(1)_A$ anomaly of strong interactions, which gives mass to the singlet η_0 in $N_C = 3$ QCD, even in the chiral limit.
- The explicit SU(3)-flavor symmetry breaking, due to the splitting $m_s \neq \hat{m}$ between the strange and up/down quark masses (the isospin limit, where $m_u = m_d = \hat{m}$ and the electromagnetic corrections are neglected, will be assumed all through the article).
- The $1/N_C$ expansion of QCD in the limit of large N_C, with N_C the number of colors in QCD.

The interaction between the pseudo-Nambu-Goldstone bosons (pNGBs) (π, K, η_8) from the spontaneous chiral symmetry breaking can be systematically described through a low-energy effective field theory (EFT) based on $\mathrm{SU}(3)_L \times \mathrm{SU}(3)_R$ chiral symmetry, namely

Chiral Perturbation Theory (χPT) [1, 2]. Following large–N_C arguments [3–5], this approach was later extended, incorporating the singlet η_0 into a U(3) χPT Lagrangian [6–14]. This combination of χPT and the $1/N_C$ expansion provides a consistent framework which addresses all the previous issues.

More precisely, in this article we show that this large–N_C χPT framework yields an excellent description of the η and η' masses from lattice simulations at different light-quark masses [15–19]. Constraints from phenomenological studies of ρ, ω, ϕ, J/ψ decays [20, 21] and kaon mass lattice simulations [22, 23] are compatible and easily accommodated in a joint fit. The problems arise when one tries to also describe lattice simulations for F_π, F_K and F_K/F_π [22–24]. Nevertheless, the issue of these observables in χPT is known and has been widely discussed in previous bibliography [25–29]. It constitutes a problem in its own and it is not the central goal of this article. It is discussed for sake of completeness and to show its impact in a global fit.

The η and η' mesons not only attract much attention from the chiral community but they have been also intensively scrutinized in lattice QCD simulations, where enormous progresses have been recently made by different groups [15–19]. Varying the light-quark masses $\hat{m}$ and m_s, both their masses and mixing angles have been extracted in the range $200\,\mathrm{MeV} < m_\pi < 700\,\mathrm{MeV}$. We will focus on the simulation points with $m_\pi < 500\,\mathrm{MeV}$ in the present work. By observing the dependence of these observables with the light-quark masses we will determine the χPT low energy constants (LECs) and further constrain the theoretical models. At the practical level we have recast all $\hat{m}$ dependencies in terms of m_π and study the observables as functions of m_π. The η and η' lattice simulations have not been thoroughly analyzed in the chiral framework yet and it is the central goal of the present work. However, the numerical uncertainties resulting from our analyses in this work must be taken with a grain of salt as correlations between the different lattice data points and other systematic errors are not considered here.

In addition to lattice QCD, there are also phenomenological studies of the η and η' mixing, which has been extensively investigated in radiative decays of light-flavor vector resonances ρ, ω, ϕ and $J/\psi \to VP, P\gamma$ processes [20, 21, 30–36]. In these works, the modern two-mixing-angle scheme for the η and η' mesons, which was first advocated in refs. [10, 11], was employed to fit various experimental data. The common methodology in these works is that the two-mixing-angle pattern for the η and η' is simply adopted to perform the phenomenological discussion and the mixing parameters are then directly determined from data. This is a bottom-up approach to address the η-η' mixing problem and it is quite useful for the phenomenological analysis. Contrary to the bottom-up method, it is also very interesting to study the η-η' mixing from a top-down approach in which one first constructs the relevant χPT Lagrangian and then calculates the η-η' mixing pattern and parameters in terms of the LECs. In this case, one can predict the η-η' mixing parameters once the values of the unknown LECs are given. The present work belongs to the latter category of top-down approaches.

Though the singlet η_0 meson, which is the main component of the physical η' state, is not a pNGB due to the strong $\mathrm{U}(1)_A$ anomaly, it can be formally introduced into χPT from the large-N_C point of view. The argument is that the quark loop induced $\mathrm{U}(1)_A$

JHEP06(2015)175

anomaly, which is responsible for the large mass of the singlet η_0, is $1/N_C$ suppressed and hence the η_0 becomes the ninth pNGB in the large N_C limit [37–39]. Based on this argument, the leading-order (LO) effective Lagrangian for U(3) χPT, which simultaneously includes the pNGB octet π, K, η_8 and the singlet η_0 as dynamical fields, was formulated in refs. [6–9]. Later on, a full $\mathcal{O}(p^4)$ U(3) chiral Lagrangian was constructed in ref. [13] and the discussion on the $\mathcal{O}(p^6)$ unitary group chiral Lagrangian has been very recently completed in ref. [40]. Subtle problems about the choice of suitable variables for the higher order U(3) χPT Lagrangian in the large N_C framework were analyzed in ref. [12].

The standard power counting employed in SU(2) and SU(3) χPT in powers of the external momenta and quark masses [1, 2], is not valid any more in U(3) χPT, due to the appearance of the large η_0 mass. However, since the singlet η_0 mass squared behaves like $1/N_C$ in large N_C limit, the η_0 mass can be harmonized with the other two expansion parameters if one assigns the same counting to $1/N_C$, the squared momenta p^2 and the light quark masses m_q. As a result of this, in order to have a systematic power counting, the combined expansions on momentum, light quark masses and $1/N_C$ are mandatory in U(3) χPT [12, 13]. We will work in this combined expansion in our study and denote it as δ expansion throughout the paper, where $\mathcal{O}(\delta) \sim \mathcal{O}(p^2) \sim \mathcal{O}(m_q) \sim \mathcal{O}(1/N_C)$. This counting rule is different from the one proposed in ref. [41], where the η_0 mass is counted as $\mathcal{O}(1)$ and the infrared regularization method is employed to handle the chiral loops.

Some recent works in refs. [14, 42–45] have addressed the η-η' mixing in the chiral framework up to next-to-leading order (NLO). As an improvement, we will perform the systematic study of the η-η' mixing in the δ-expansion scheme up to next-to-next-to-leading order (NNLO) and take into account the very recent lattice simulation data, which are not considered in the previous works [14, 42–45]. In addition, we also simultaneously analyze the m_π dependences of other physical quantities from lattice simulations, such as the axial π, K decay constants and the mass ratio of the strange and up/down quarks, in order to further constrain the χPT LECs.

This article is organized as follows. In section 2, we introduce the theoretical framework and calculate the relevant physical quantities. In section 3, the phenomenological discussions will be presented. Conclusions will be given in section 4. Further details about the calculations up to NNLO are relegated to appendix A.

2 Theoretical framework

2.1 Relevant chiral Lagrangian

At leading order in the δ expansion, i.e. $\mathcal{O}(\delta^0)$, the U(3) χPT Lagrangian consists of three operators

$$\mathcal{L}^{(\delta^0)} = \frac{F^2}{4}\langle u_\mu u^\mu\rangle + \frac{F^2}{4}\langle\chi_+\rangle + \frac{F^2}{12}M_0^2 X^2\,, \tag{2.1}$$

where the chiral building blocks are defined as [1, 2, 12–14]

$$\begin{aligned} U &= u^2 = e^{i\frac{\sqrt{2}\Phi}{F}}\,, \qquad \chi = 2B(s+ip)\,, \qquad \chi_\pm = u^\dagger\chi u^\dagger \pm u\chi^\dagger u\,, \qquad X = \log(\det U)\,,\\ u_\mu &= iu^\dagger D_\mu U u^\dagger\,, \qquad D_\mu U = \partial_\mu U - i(v_\mu + a_\mu)U + iU(v_\mu - a_\mu)\,, \end{aligned} \tag{2.2}$$

JHEP06(2015)175

with the pNGB octet+singlet matrix

$$\Phi = \begin{pmatrix} \frac{1}{\sqrt{2}}\pi^0 + \frac{1}{\sqrt{6}}\eta_8 + \frac{1}{\sqrt{3}}\eta_0 & \pi^+ & K^+ \\ \pi^- & \frac{-1}{\sqrt{2}}\pi^0 + \frac{1}{\sqrt{6}}\eta_8 + \frac{1}{\sqrt{3}}\eta_0 & K^0 \\ K^- & \overline{K}^0 & \frac{-2}{\sqrt{6}}\eta_8 + \frac{1}{\sqrt{3}}\eta_0 \end{pmatrix}, \tag{2.3}$$

and s, p, v_μ, a_μ being the external scalar, pseudoscalar, vector and axial-vector sources, respectively. The coupling F appearing in eqs.(2.1) and (2.2) corresponds to the pNGB axial decay constant in the large N_C and chiral limits. The light quark masses are introduced by setting $(s+ip)$ =diag$\{\hat{m}, \hat{m}, m_s\}$, being $\hat{m}$ the averaged up and down quark masses and m_s that of the strange quark.

Notice the structure of the LO Lagrangian in eq. (2.1): the first operator is of $\mathcal{O}(N_C, p^2)$ type, the second one corresponds to the type of $\mathcal{O}(N_C, m_q)$ and the last one stems from the QCD U(1)$_A$ anomaly and is of $\mathcal{O}(N_C^0, p^0)$ type, where U is counted as $\mathcal{O}(1)$,$F^2 \sim \mathcal{O}(N_C)$ and $M_0^2 \sim \mathcal{O}(N_C^{-1})$ in the classification $\mathcal{O}(N_C^j, p^k, m_q^\ell)$ of the EFT Lagrangian operators in eq. (2.1). In the following, we will denote the chiral expansions in powers of squared momenta p^2 and quark masses m_q simply as a generic expansion in p^2.

The NLO U(3) chiral Lagrangian, i.e., $\mathcal{O}(\delta)$, contains $\mathcal{O}(N_C, p^4)$ and $\mathcal{O}(N_C^0, p^2)$ operators. The relevant ones in our work read [12]

$$\mathcal{L}^{(\delta)} = L_5\langle u^\mu u_\mu \chi_+\rangle + \frac{L_8}{2}\langle \chi_+\chi_+ + \chi_-\chi_-\rangle + \frac{F^2\,\Lambda_1}{12} D^\mu X D_\mu X - \frac{F^2\,\Lambda_2}{12} X\langle \chi_-\rangle\,, \tag{2.4}$$

with the dimensionless LECs' scaling like $L_5, L_8 \sim \mathcal{O}(N_C)$ and $\Lambda_1, \Lambda_2 \sim \mathcal{O}(N_C^{-1})$.

At NNLO, i.e. $\mathcal{O}(\delta^2)$, there are three types of operators: $\mathcal{O}(N_C^{-1}, p^2)$, $\mathcal{O}(N_C^0, p^4)$ and $\mathcal{O}(N_C, p^6)$. Their explicit forms read [13, 46]

$$\begin{aligned} \mathcal{L}^{(\delta^2)} = {} & \frac{F^2\, v_2^{(2)}}{4} X^2\langle \chi_+\rangle \\ & + L_4\langle u^\mu u_\mu\rangle\langle \chi_+\rangle + L_6\langle \chi_+\rangle\langle \chi_+\rangle + L_7\langle \chi_-\rangle\langle \chi_-\rangle + L_{18}\langle u_\mu\rangle\langle u^\mu \chi_+\rangle + L_{25} X\langle \chi_+\chi_-\rangle \\ & + C_{12}\langle h_{\mu\nu}h^{\mu\nu}\chi_+\rangle + C_{14}\langle u_\mu u^\mu \chi_+\chi_+\rangle + C_{17}\langle u_\mu \chi_+ u^\mu \chi_+\rangle \\ & + C_{19}\langle \chi_+\chi_+\chi_+\rangle + C_{31}\langle \chi_-\chi_-\chi_+\rangle\,, \end{aligned} \tag{2.5}$$

where the first line corresponds to the $\mathcal{O}(N_C^{-1}, p^2)$ type, the second line is of the $\mathcal{O}(N_C^0, p^4)$ type and the last two lines are of the $\mathcal{O}(N_C, p^6)$ type. The LECs carry the scalings $v_2^{(2)} \sim \mathcal{O}(N_C^{-2})$, $L_4, L_6, L_7, L_{18}, L_{25} \sim \mathcal{O}(N_C^0)$ and $C_{12}, C_{14}, C_{17}, C_{19}, C_{31} \sim \mathcal{O}(N_C)$. Notice that we have only shown the operators at different δ orders in eqs. (2.1), (2.4) and (2.5) that are pertinent to our present study, not aiming at giving the complete sets of operators. The conventions to label the LO, NLO and NNLO operators in eqs. (2.1), (2.4) and (2.5) follow closely the notations in refs. [12, 13, 46]. Unless it is explicitly stated, the LECs will correspond to U(3) χPT and must not be confused with those in SU(3) χPT. The matching between these two EFTs can be found in ref. [12]. The terms L_j are denoted as β_j in refs. [13, 14].

Comparing the U(3) and SU(3) theories one can observe that some terms have been reshuffled in the δ expansion of the U(3) Lagrangian. For example, the $L_{i=4,5,6,7,8}$ terms are NLO in SU(3) χPT, but they are now split into NLO and NNLO in the δ expansion

JHEP06(2015)175

(see eqs. (2.4) and (2.5)). We have several additional new operators, namely the last one in eq. (2.1), the $\Lambda_{i=1,2}$ in eq. (2.4) and the $v_2^{(2)}, L_{18}, L_{25}$ terms in eq. (2.5), that are absent in the SU(3) χPT case. Finally, the chiral loops start contributing at NNLO in the δ expansion, while they appear at NLO in the conventional SU(3) case.

2.2 The η-η' mixing at NNLO in δ expansion

Next we calculate the η-η' mixing order by order in the δ expansion. In literature, there are two bases to address the η-η' mixing, namely the singlet-octet basis with η_0 and η_8, and the quark-flavor basis with η_q and η_s. The relations between fields in these two bases are

$$\begin{pmatrix} \eta_8 \\ \eta_0 \end{pmatrix} = \begin{pmatrix} \sqrt{\frac{1}{3}} & -\sqrt{\frac{2}{3}} \\ \sqrt{\frac{2}{3}} & \sqrt{\frac{1}{3}} \end{pmatrix} \begin{pmatrix} \eta_q \\ \eta_s \end{pmatrix} . \tag{2.6}$$

In the large–N_C limit where the $\mathrm{U}(1)_A$ anomaly is absent, η_q and η_s are the mass eigenstates and they are generated by the axial-vector currents with the quark flavors $q\bar{q} = (u\bar{u} + d\bar{d})/\sqrt{2}$ and $s\bar{s}$, respectively. The two bases are related to each other through an orthogonal transformation and provide an equivalent description for the η-η' mixing.

As noticed in refs. [45, 47], when doing the loop calculations with η and η', it is rather cumbersome to work with the η_0 and η_8 states. The reason is that at leading order the Lagrangian in eq. (2.1) gives the mixing between η_0 and η_8, and the mixing strength is proportional to $m_K^2 - m_\pi^2$, which in the δ expansion is formally counted as the same order as the diagonal terms in the mass matrix for η_0 and η_8. As a result, the insertion of the η_0-η_8 mixing in the chiral loops will not increase the δ order of the loop diagrams. This makes the loop calculation technically much more complicated, as one needs to consider the arbitrary insertions of the η_0-η_8 mixing in the chiral loop diagrams. Nevertheless, refs. [45, 47] provide a simple recipe to handle this problem by expressing the Lagrangian in terms of the $\overline{\eta}$ and $\overline{\eta}'$ states which result from the diagonalization of η_0 and η_8 at leading order in δ. The main difference is that the mixing between $\overline{\eta}$ and $\overline{\eta}'$ is now at least a NLO effect in δ, while the η_0-η_8 mixing was appearing at LO. The relation between the LO mass eigenstates $\bar{\eta}$ and $\bar{\eta}'$ and the singlet-octet basis is given by the mixing angle θ:

$$\begin{pmatrix} \bar{\eta} \\ \bar{\eta}' \end{pmatrix} = \begin{pmatrix} c_\theta & -s_\theta \\ s_\theta & c_\theta \end{pmatrix} \begin{pmatrix} \eta_8 \\ \eta_0 \end{pmatrix} , \tag{2.7}$$

with $c_\theta = \cos\theta$ and $s_\theta = \sin\theta$. The LO mixing angle θ and masses of $\overline{\eta}$ and $\overline{\eta}'$ are given by the leading order Lagrangian $\mathcal{L}^{(\delta^0)}$ in eq. (2.1) (see e.g. ref. [45]):

$$m_{\overline{\eta}}^2 = \frac{M_0^2}{2} + \overline{m}_K^2 - \frac{\sqrt{M_0^4 - \frac{4M_0^2\Delta^2}{3} + 4\Delta^4}}{2} , \tag{2.8}$$

$$m_{\overline{\eta}'}^2 = \frac{M_0^2}{2} + \overline{m}_K^2 + \frac{\sqrt{M_0^4 - \frac{4M_0^2\Delta^2}{3} + 4\Delta^4}}{2} , \tag{2.9}$$

$$\sin\theta = -\left(\sqrt{1 + \frac{\left(3M_0^2 - 2\Delta^2 + \sqrt{9M_0^4 - 12M_0^2\Delta^2 + 36\Delta^4}\right)^2}{32\Delta^4}} \right)^{-1} , \tag{2.10}$$

with $\Delta^2 = \overline{m}_K^2 - \overline{m}_\pi^2$. Here $\overline{m}_K$ and $\overline{m}_\pi$ denote the LO kaon and pion masses, respectively.

JHEP06(2015)175

When higher order corrections are taken into account, the LO diagonalized $\overline{\eta}$ and $\overline{\eta}'$ will get mixed again. Up to the NNLO, a general parametrization of the bilinear terms involving the $\overline{\eta}$ and $\overline{\eta}'$ states can be written as

$$\begin{aligned}\mathcal{L} = & \frac{\delta_1}{2}\,\partial_\mu\partial_\nu\overline{\eta}\partial^\mu\partial^\nu\overline{\eta} + \frac{\delta_2}{2}\,\partial_\mu\partial_\nu\overline{\eta}'\partial^\mu\partial^\nu\overline{\eta}' + \delta_3\,\partial_\mu\partial_\nu\overline{\eta}\partial^\mu\partial^\nu\overline{\eta}' \\ & + \frac{1+\delta_{\overline{\eta}}}{2}\partial_\mu\overline{\eta}\partial^\mu\overline{\eta} + \frac{1+\delta_{\overline{\eta}'}}{2}\partial_\mu\overline{\eta}'\partial^\mu\overline{\eta}' + \delta_k\,\partial_\mu\overline{\eta}\partial^\mu\overline{\eta}' \\ & - \frac{m_{\overline{\eta}}^2+\delta_{m_{\overline{\eta}}^2}}{2}\overline{\eta}\,\overline{\eta} - \frac{m_{\overline{\eta}'}^2+\delta_{m_{\overline{\eta}'}^2}}{2}\overline{\eta}'\overline{\eta}' - \delta_{m^2}\,\overline{\eta}\,\overline{\eta}'\,, \end{aligned} \tag{2.11}$$

where the $\delta_i's$ contain the NLO and NNLO corrections. Here these operators must be understood as the terms of the effective action that provide the pseudoscalar meson self-energies. The higher-derivative terms $\delta_{j=1,2,3}$ in the first line of eq. (2.11) are exclusively contributed by the $\mathcal{O}(p^6)$ operator C_{12} in eq. (2.5), which belongs to the NNLO Lagrangian. The remaining $\delta_i's$ receive contributions from the NLO operators in eq. (2.4), the NNLO ones in eq. (2.5) and the one-loop diagrams, which contribute at NNLO. Their explicit expressions can be found in appendix A.

At leading order, there is only the mass mixing term from eq. (2.1) whereas at NLO and NNLO one has to deal in addition with the kinematic mixing terms in eq. (2.11), apart from the mass mixing. The physical states of η and η' can be obtained from the perturbative-expansion (δ-expansion) in three steps: as a first step, we eliminate the higher-derivative terms through the field redefinitions of $\overline{\eta}$ and $\overline{\eta}'$; then we transform and rescale the fields resulting from the first step in order to write the kinematic terms in the canonical form; after the preceding two steps, there is only the mass mixing term left, which is straightforward to handle.

In the first step, we make the following field redefinitions for the $\overline{\eta}$ and $\overline{\eta}'$ states

$$\overline{\eta} \to \overline{\eta} + \alpha_1\Box\overline{\eta} + \alpha_2\Box\overline{\eta}'\,, \quad \overline{\eta}' \to \overline{\eta}' + \alpha_2\Box\overline{\eta} + \alpha_3\Box\overline{\eta}'\,, \tag{2.12}$$

with the d'Alembert operator $\Box \equiv \partial_\mu\partial^\mu$. After some algebra manipulations, it is straightforward to obtain

$$\alpha_1 = -\frac{\delta_1}{2}\,, \qquad \alpha_2 = -\frac{\delta_3}{2}\,, \qquad \alpha_3 = -\frac{\delta_2}{2}\,, \tag{2.13}$$

so that the three higher-derivative terms in eq. (2.11) will be eliminated. Notice that the $\alpha_{1,2,3}$ are NNLO, i.e., $\mathcal{O}(\delta^2)$. Substituting the field redefinitions from eq. (2.12) into the general mixing structure in eq. (2.11) and keeping the terms up to NNLO, the resulting bilinear Lagrangian reads

$$\begin{aligned}\mathcal{L} = & \frac{1+\delta_{\overline{\eta}}+m_{\overline{\eta}}^2\delta_1}{2}\partial_\mu\overline{\eta}\partial^\mu\overline{\eta} + \frac{1+\delta_{\overline{\eta}'}+m_{\overline{\eta}'}^2\,\delta_2}{2}\partial_\mu\overline{\eta}'\partial^\mu\overline{\eta}' + \left[\delta_k + \frac{\delta_3}{2}(m_{\overline{\eta}}^2+m_{\overline{\eta}'}^2)\right]\partial_\mu\overline{\eta}\partial^\mu\overline{\eta}' \\ & - \frac{m_{\overline{\eta}}^2+\delta_{m_{\overline{\eta}}^2}}{2}\overline{\eta}\,\overline{\eta} - \frac{m_{\overline{\eta}'}^2+\delta_{m_{\overline{\eta}'}^2}}{2}\overline{\eta}'\overline{\eta}' - \delta_{m^2}\,\overline{\eta}\,\overline{\eta}'\,. \end{aligned} \tag{2.14}$$

In the second step, we need to eliminate the kinematic mixing term in eq. (2.14), and then to rescale the fields to have them in the canonical forms. This can be done

JHEP06(2015)175

perturbatively. In the final step, we take care of the mass mixing term. The last two steps can be achieved through the following field transformations

$$\begin{pmatrix} \eta \\ \eta' \end{pmatrix} = \begin{pmatrix} \cos\theta_\delta & -\sin\theta_\delta \\ \sin\theta_\delta & \cos\theta_\delta \end{pmatrix} \begin{pmatrix} 1+\delta_A & \delta_B \\ \delta_B & 1+\delta_C \end{pmatrix} \begin{pmatrix} \overline{\eta} \\ \overline{\eta}' \end{pmatrix} , \tag{2.15}$$

with η, η' the physical states and

$$\begin{aligned} \delta_A &= \frac{\delta_{\overline{\eta}}}{2} + \frac{m_{\overline{\eta}}^2 \delta_1}{2} - \frac{\delta_{\overline{\eta},\mathrm{NLO}}^2}{8} - \frac{\delta_{k,\mathrm{NLO}}^2}{8} , \\ \delta_B &= \frac{\delta_k}{2} + \frac{\delta_3}{4}(m_{\overline{\eta}}^2 + m_{\overline{\eta}'}^2) - \frac{\delta_{\overline{\eta},\mathrm{NLO}}\delta_{k,\mathrm{NLO}}}{8} - \frac{\delta_{\overline{\eta}',\mathrm{NLO}}\delta_{k,\mathrm{NLO}}}{8} , \\ \delta_C &= \frac{\delta_{\overline{\eta}'}}{2} + \frac{m_{\overline{\eta}'}^2 \delta_2}{2} - \frac{\delta_{\overline{\eta}',\mathrm{NLO}}^2}{8} - \frac{\delta_{k,\mathrm{NLO}}^2}{8} , \end{aligned} \tag{2.16}$$

where $\delta_{\overline{\eta},\mathrm{NLO}}, \delta_{\overline{\eta}',\mathrm{NLO}}, \delta_{k,\mathrm{NLO}}$ stand for the NLO parts of the three quantities respectively. We point out that $\delta_{\overline{\eta}}, \delta_{\overline{\eta}'}, \delta_k$ receive both NLO and NNLO contributions, while $\delta_1, \delta_2, \delta_3$ are only contributed by the NNLO effect, which is the C_{12} operator in eq. (2.5). Comparing with the NLO results in eq. (15) from our previous paper [45], we have generalized the expression to the NNLO case in the present eq. (2.15). Another way to treat the mixing of pseudoscalar mesons in χPT was also previously studied in ref. [48] and applied to the π^0-η case up to the two-loop level.

In the practical calculation, it is more often to use the inverse of the relations in eq. (2.15), where the perturbative expansion leads to

$$\begin{pmatrix} \overline{\eta} \\ \overline{\eta}' \end{pmatrix} = \begin{pmatrix} 1+\delta'_A & \delta'_B \\ \delta'_B & 1+\delta'_C \end{pmatrix} \begin{pmatrix} \cos\theta_\delta & \sin\theta_\delta \\ -\sin\theta_\delta & \cos\theta_\delta \end{pmatrix} \begin{pmatrix} \eta \\ \eta' \end{pmatrix} , \tag{2.17}$$

with

$$\begin{aligned} \delta'_A &= -\frac{\delta_{\overline{\eta}}}{2} - \frac{m_{\overline{\eta}}^2 \delta_1}{2} + \frac{3\delta_{\overline{\eta},\mathrm{NLO}}^2}{8} + \frac{3\delta_{k,\mathrm{NLO}}^2}{8} , \\ \delta'_B &= -\frac{\delta_k}{2} - \frac{\delta_3}{4}(m_{\overline{\eta}}^2 + m_{\overline{\eta}'}^2) + \frac{3\delta_{\overline{\eta},\mathrm{NLO}}\delta_{k,\mathrm{NLO}}}{8} + \frac{3\delta_{\overline{\eta}',\mathrm{NLO}}\delta_{k,\mathrm{NLO}}}{8} , \\ \delta'_C &= -\frac{\delta_{\overline{\eta}'}}{2} - \frac{m_{\overline{\eta}'}^2 \delta_2}{2} + \frac{3\delta_{\overline{\eta}',\mathrm{NLO}}^2}{8} + \frac{3\delta_{k,\mathrm{NLO}}^2}{8} . \end{aligned} \tag{2.18}$$

The θ_δ appearing in eqs. (2.15) and (2.17) is determined through

$$\tan\theta_\delta = \frac{\widehat{\delta}_{m^2}}{m_{\eta'}^2 - \widehat{m}_\eta^2} , \tag{2.19}$$

JHEP06(2015)175

with

$$
\begin{aligned}
\widehat{\delta}_{m^2} &= \delta_{m^2} - \frac{1}{2}\left[\delta_k + \frac{\delta_3}{2}(m_{\overline{\eta}}^2 + m_{\overline{\eta}'}^2)\right]\left(m_{\overline{\eta}}^2 + m_{\overline{\eta}'}^2\right) + \frac{1}{8}\delta_{k,\mathrm{NLO}}\delta_{\overline{\eta},\mathrm{NLO}}\left(5m_{\overline{\eta}}^2 + 3m_{\overline{\eta}'}^2\right) \\
&\quad -\frac{1}{2}\delta_{k,\mathrm{NLO}}\left(\delta_{m_{\overline{\eta}}^2,\mathrm{NLO}} + \delta_{m_{\overline{\eta}'}^2,\mathrm{NLO}}\right) + \frac{1}{8}\delta_{k,\mathrm{NLO}}\delta_{\overline{\eta}',\mathrm{NLO}}\left(3m_{\overline{\eta}}^2 + 5m_{\overline{\eta}'}^2\right) \\
&\quad -\frac{1}{2}\delta_{m^2,\mathrm{NLO}}\left(\delta_{\overline{\eta},\mathrm{NLO}} + \delta_{\overline{\eta}',\mathrm{NLO}}\right) , \\
\widehat{m}_\eta^2 &= m_{\overline{\eta}}^2 + \delta_{m_{\overline{\eta}}^2} - m_{\overline{\eta}}^2\left(\delta_{\overline{\eta}} + m_{\overline{\eta}}^2\delta_1\right) + m_{\overline{\eta}}^2\delta_{\overline{\eta},\mathrm{NLO}}^2 + \frac{3}{4}m_{\overline{\eta}}^2\delta_{k,\mathrm{NLO}}^2 + \frac{1}{4}m_{\overline{\eta}'}^2\delta_{k,\mathrm{NLO}}^2 \\
&\quad -\delta_{k,\mathrm{NLO}}\delta_{m^2,\mathrm{NLO}} - \delta_{\overline{\eta},\mathrm{NLO}}\delta_{m_{\overline{\eta}}^2,\mathrm{NLO}} , \\
\widehat{m}_{\eta'}^2 &= m_{\overline{\eta}'}^2 + \delta_{m_{\overline{\eta}'}^2} - m_{\overline{\eta}'}^2\left(\delta_{\overline{\eta}'} + m_{\overline{\eta}'}^2\delta_2\right) + m_{\overline{\eta}'}^2\delta_{\overline{\eta}',\mathrm{NLO}}^2 + \frac{1}{4}m_{\overline{\eta}}^2\delta_{k,\mathrm{NLO}}^2 + \frac{3}{4}m_{\overline{\eta}'}^2\delta_{k,\mathrm{NLO}}^2 \\
&\quad -\delta_{k,\mathrm{NLO}}\delta_{m^2,\mathrm{NLO}} - \delta_{\overline{\eta}',\mathrm{NLO}}\delta_{m_{\overline{\eta}'}^2,\mathrm{NLO}} , \\
2m_\eta^2 &= \widehat{m}_\eta^2 + \widehat{m}_{\eta'}^2 - \sqrt{\left(\widehat{m}_\eta^2 - \widehat{m}_{\eta'}^2\right)^2 + 4\widehat{\delta}_{m^2}^2} , \\
2m_{\eta'}^2 &= \widehat{m}_\eta^2 + \widehat{m}_{\eta'}^2 + \sqrt{\left(\widehat{m}_\eta^2 - \widehat{m}_{\eta'}^2\right)^2 + 4\widehat{\delta}_{m^2}^2} ,
\end{aligned}
\tag{2.20}
$$

where $\delta_{i,\mathrm{NLO}}$ stand for the NLO parts of δ_i.

In the phenomenological discussions, the popular two-mixing-angle parametrization in the singlet-octet basis [10, 11] takes the form

$$
\begin{pmatrix} \eta \\ \eta' \end{pmatrix} = \frac{1}{F}\begin{pmatrix} F_8\cos\theta_8 & -F_0\sin\theta_0 \\ F_8\sin\theta_8 & F_0\cos\theta_0 \end{pmatrix}\begin{pmatrix} \eta_8 \\ \eta_0 \end{pmatrix} . \tag{2.21}
$$

Combining eqs. (2.7) and (2.15), it is straightforward to derive the relations between the four parameters in the two-mixing-angle scheme in eq. (2.21) and the χPT LECs:

$$
\begin{aligned}
F_8^2 &= F^2\Big\{\big[\cos(\theta+\theta_\delta) + \delta_B\sin(\theta-\theta_\delta) + \delta_A\cos\theta\cos\theta_\delta - \delta_C\sin\theta\sin\theta_\delta\big]^2 \\
&\quad +\big[\sin(\theta+\theta_\delta) + \delta_B\cos(\theta-\theta_\delta) + \delta_A\cos\theta\sin\theta_\delta + \delta_C\sin\theta\cos\theta_\delta\big]^2\Big\} , \\
F_0^2 &= F^2\Big\{\big[-\sin(\theta+\theta_\delta) + \delta_B\cos(\theta-\theta_\delta) - \delta_A\sin\theta\cos\theta_\delta - \delta_C\cos\theta\sin\theta_\delta\big]^2 \\
&\quad +\big[\cos(\theta+\theta_\delta) - \delta_B\sin(\theta-\theta_\delta) - \delta_A\sin\theta\sin\theta_\delta + \delta_C\cos\theta\cos\theta_\delta\big]^2\Big\} , \\
\tan\theta_8 &= \frac{\sin(\theta+\theta_\delta) + \delta_B\cos(\theta-\theta_\delta) + \delta_A\cos\theta\sin\theta_\delta + \delta_C\sin\theta\cos\theta_\delta}{\cos(\theta+\theta_\delta) + \delta_B\sin(\theta-\theta_\delta) + \delta_A\cos\theta\cos\theta_\delta - \delta_C\sin\theta\sin\theta_\delta} , \\
\tan\theta_0 &= -\frac{-\sin(\theta+\theta_\delta) + \delta_B\cos(\theta-\theta_\delta) - \delta_A\sin\theta\cos\theta_\delta - \delta_C\cos\theta\sin\theta_\delta}{\cos(\theta+\theta_\delta) - \delta_B\sin(\theta-\theta_\delta) - \delta_A\sin\theta\sin\theta_\delta + \delta_C\cos\theta\cos\theta_\delta} ,
\end{aligned}
\tag{2.22}
$$

where the χPT LECs are implicitly included in θ, θ_δ, δ_A, δ_B and δ_C. Since $\theta_\delta, \delta_A, \delta_B, \delta_C \sim \mathcal{O}(\delta)$ or $\mathcal{O}(\delta^2)$, at LO one has $F_8 = F_0 = F$ and one mixing-angle $\theta_8 = \theta_0 = \theta$.

JHEP06(2015)175

The relations between the physical η, η' states and the quark-flavor basis is commonly parametrized as

$$\begin{pmatrix} \eta \\ \eta' \end{pmatrix} = \frac{1}{F} \begin{pmatrix} F_q \cos\phi_q & -F_s \sin\phi_s \\ F_q \sin\phi_q & F_s \cos\phi_s \end{pmatrix} \begin{pmatrix} \eta_q \\ \eta_s \end{pmatrix} . \tag{2.23}$$

Combining eqs. (2.6), (2.7) and (2.15), it is straightforward to obtain the parameters in eq. (2.23):

$$\begin{aligned} F_q^2 &= \frac{2F_0^2 + F_8^2 - 2\sqrt{2}F_0F_8\sin(\theta_0 - \theta_8)}{3} , \\ F_s^2 &= \frac{F_0^2 + 2F_8^2 + 2\sqrt{2}F_0F_8\sin(\theta_0 - \theta_8)}{3} , \\ \tan\phi_q &= \frac{\sqrt{2}F_8\cos\theta_8 + F_0\sin\theta_0}{\sqrt{2}F_0\sin\theta_0 - F_8\cos\theta_8} , \\ \tan\phi_s &= \frac{\sqrt{2}F_0\cos\theta_0 + F_8\sin\theta_8}{\sqrt{2}F_8\sin\theta_8 - F_0\cos\theta_0} , \end{aligned} \tag{2.24}$$

where at LO in the δ-expansion one has $F_q = F_s = F$ and $\phi_q = \phi_s = \theta_{\rm id} - \theta$, with the ideal mixing $\theta_{\rm id} = -\arcsin\sqrt{2/3}$.

2.3 Insights into previous studies of the η-η' mixing

In the previous subsection we have performed the full computation of the mixing up to NNLO in the δ expansion. It is interesting to make a brief summary of the assumptions made in previous works, where plenty of mixing formalisms have been proposed to address the η-η' system [14, 30, 42–45, 49, 50]. In ref. [49], only the lowest order in the quark masses and $1/N_C$, i.e. the LO contributions in the δ expansion, were taken into account. Even though it provided a reasonable first approximation, it failed to give an accurate description of the experimentally observed mass ratio $m_\eta^2/m_{\eta'}^2$. The $\mathcal{O}(p^2)$ contributions were studied up to NLO in $1/N_C$ in ref. [50] (including the terms in eq. (2.1) and Λ_1 and Λ_2 in eq. (2.4)), perfectly explaining the experimental value of $m_\eta^2/m_{\eta'}^2$. However, it turned out to be inadequate to give a proper value for the η-η' mixing angle. On the other hand, the authors in refs. [42–44] went up to NLO in the p^2 expansion but keeping just the LO in $1/N_C$ (including the terms in eq. (2.1) and L_5 and L_8 in eq. (2.4)). Both the η-η' mixing angle and the ratio F_K/F_π were qualitatively reproduced in this case. The full set of NLO contributions in the δ-expansion (i.e., the effects up to NLO both in $1/N_C$ and p^2) was analyzed in ref. [14], together with the mixing angle and the π, K, η and η' axial-vector decay constants. In ref. [45], the contributions from the tree-level resonance exchanges and partial NNLO effects, e.g. the loop diagrams, were considered for the masses of η and η'. In this work, we generalize the discussions up to the full NNLO study in the δ-expansion and confront our theoretical expressions with the very recent lattice simulation data and the phenomenological inputs from the two-mixing-angle scheme.

Reference [30] introduced a quark-model inspired approach to the η-η' mixing, which is commonly referred as the FKS formalism and used in many phenomenological analyses [51].

JHEP06(2015)175

The essence of the FKS formalism is the assumption that the axial decay constants in the quark-flavor basis takes the same mixing pattern as the states

$$\begin{pmatrix} F_\eta^q & F_\eta^s \\ F_{\eta'}^q & F_{\eta'}^s \end{pmatrix} = \begin{pmatrix} \cos\phi & -\sin\phi \\ \sin\phi & \cos\phi \end{pmatrix} \begin{pmatrix} F_q & 0 \\ 0 & F_s \end{pmatrix} , \tag{2.25}$$

where the decay constants are defined as the matrix elements of the axial currents

$$\begin{aligned} \langle 0|A_\mu^a(0)|P(k)\rangle &= i\sqrt{2}F_P^a k_\mu , & (a = q, s; P = \eta, \eta') , \\ A_\mu^q &= \frac{1}{\sqrt{2}}\big(\bar{u}\gamma_\mu\gamma_5 u + \bar{d}\gamma_\mu\gamma_5 d\big) , & A_\mu^s = \bar{s}\gamma_\mu\gamma_5 s . \end{aligned} \tag{2.26}$$

From another point of view, the pattern of eq. (2.25) employed in the FKS formalism relies on the assumption that there is no mixing between the decay constants of the flavor states η_q and η_s. In the χPT framework, the physical masses and decay constants can be obtained from the bilinear parts of nonet fields in the effective action with the correlation function of two axial currents. Since the correlation function is the second derivative with respect to the axial-vector external source a_μ, and a_μ always appears in the Lagrangian together with the partial derivative ∂_μ as shown in eq. (2.2), the absence of the mixing for the η_q and η_s decay constants in eq. (2.25) implies that there are no kinematic mixing terms for the quark-flavor states η_q and η_s in the FKS formalism. In fact, the assumption in ref. [42] is in accord with the FKS formalism. This can be simply demonstrated by expanding the chiral operators considered in refs. [42, 43], i.e. those in eq. (2.1) and L_5, L_8 in eq. (2.4), up to quadratic terms in η_q and η_s.[1] No kinematic mixing terms for the η_q and η_s fields result from these chiral operators. This also confirms the finding in ref. [44] that only when the NLO of $1/N_C$ operator is excluded the FKS formalism is recovered with their chiral Lagrangian calculations.

Since general terms up to NNLO in δ expansion are kept in our discussion, unlike in the previous works [14, 42–45, 49, 50] where different assumptions, such as the preference of the higher order p^2 and $1/N_C$ effects, are made, it is important and interesting for us to justify these assumptions in later discussions.

2.4 Masses and decay constants of pion and kaon up to NNLO in δ expansion

The NLO expression of the pion decay constant in the δ expansion reads

$$F_\pi = F\left(1 + 4L_5\frac{m_\pi^2}{F^2}\right) , \tag{2.27}$$

or, up to the precision considered, one can also use the physical F_π in the expression inside brackets,

$$F_\pi = F\left(1 + 4L_5\frac{m_\pi^2}{F_\pi^2}\right) . \tag{2.28}$$

[1] Our L_5 and L_8 operators correspond to the Λ_2 and Λ_1 terms in refs. [42–44], respectively. The Λ term in the previous references corresponds to our Λ_2 operator in eq. (2.4). The Λ term, though introduced from the beginning in these references, is dropped in their later discussions, since it is $1/N_C$ suppressed.

JHEP06(2015)175

The differences between eqs. (2.27) and (2.28) are NNLO effects. We mention that at a given order there is always ambiguity in choosing the renormalized quantities in the higher order expressions. In contrast, there is formally no ambiguity in the expressions in terms of the quantity F, which is the pNGB axial decay constant in the chiral and large N_C limits. For example, if we limit our analysis up to NLO, formally, it is equally good to use F_π or F_K in the denominators of the NLO part in eq. (2.28), since the difference is beyond the NLO precision. A typical solution in the chiral study is to express the quantities, such as m_π, F_π, m_K, F_K, in terms of the renormalized F_π in the higher order corrections, as done in the two-loop calculations in SU(3) χPT [52]. We follow this rule throughout the current work to estimate the uncertainty due to the truncation of the δ expansion when one works at a given order in perturbation theory. We mention that the notation of m_π^2 in the above equations stands for the renormalized pion mass squared and the leading order mass squared is denoted by $\overline{m}_\pi^2$. Notice the LO pion mass squared $\overline{m}_\pi^2$ is the one that is linear in the quark masses. The expressions relating m_π^2 and $\overline{m}_\pi^2$ will be discussed below.

Similarly up to NNLO, we can either use F or F_π in the NLO and NNLO expressions for other quantities such as F_K and the δ_i's in eq. (2.11). In the NNLO expressions, the difference between using F or F_π in the denominators is a next-to-next-to-next-to-leading order effect (N^{3}LO). Since in this work we study lattice simulation data up to pion mass of 500 MeV, the convergence of the chiral series is expected to be much slower than that in the physical case with $m_\pi = 135$ MeV. Therefore it is *a priori* not trivial to judge whether the two approaches–using $1/F^2$ and $1/F_\pi^2$– are numerically equivalent or the lattice data prefer one of them. Indeed in ref. [53], it is already noticed that to use F or F_π could cause some noticeable effects. We will use the difference between both approaches as an estimate of the truncation error at a given order in δ.

We take the pion decay constant as an example to illustrate the differences of using F and F_π in the higher order expressions. Using F in the higher order corrections, its expression reads

$$F_\pi = F\Bigg[1 + 4L_5\frac{m_\pi^2}{F^2} + 4L_4\frac{m_\pi^2+2m_K^2}{F^2} + (24L_5^2 - 64L_5L_8)\frac{m_\pi^4}{F^4} + (8C_{14}+8C_{17})\frac{m_\pi^4}{F^2} + \frac{A_0(m_\pi^2)}{16\pi^2F^2} + \frac{A_0(m_K^2)}{32\pi^2F^2}\Bigg]. \tag{2.29}$$

The one-point loop function $A_0(m^2)$ is calculated in dimensional regularization within the $\overline{MS}-1$ scheme [1, 2] and it reads

$$A_0(m^2) = -m^2\ln\frac{m^2}{\mu^2}\,, \tag{2.30}$$

with the renormalization scale μ fixed at 770 MeV throughout. Using eq. (2.27) to replace F by F_π in the NLO and NNLO corrections, the resulting form is

$$F_\pi = F\Bigg[1 + 4L_5\frac{m_\pi^2}{F_\pi^2} + 4L_4\frac{m_\pi^2+2m_K^2}{F_\pi^2} + (56L_5^2 - 64L_5L_8)\frac{m_\pi^4}{F_\pi^4} + (8C_{14}+8C_{17})\frac{m_\pi^4}{F_\pi^2} + \frac{A_0(m_\pi^2)}{16\pi^2F_\pi^2} + \frac{A_0(m_K^2)}{32\pi^2F_\pi^2}\Bigg]. \tag{2.31}$$

JHEP06(2015)175

In the δ expansion, the expressions for a physical quantity with F or F_π in the higher order chiral corrections differ only for the $L_5 L_{j=5,8}$ and $L_5 \Lambda_{j=1,2}$ terms, since the differences by replacing F by F_π are originated from the NLO expressions of F_π in eq. (2.28) and we only retain terms up to NNLO in this work. It is clear that the difference between eqs. (2.29) and (2.31) is the L_5^2 term. Notice that in the δ expansion scheme, the terms like $L_5 L_4$ are N^{3}LO and will be dropped throughout the article.

The corresponding expression for the kaon decay constant when one uses F to express the NLO and NNLO corrections reads

$$F_K = F\Bigg[1+4L_5\frac{m_K^2}{F^2}+4L_4\frac{m_\pi^2+2m_K^2}{F^2}+(24L_5^2-64L_5L_8)\frac{m_K^4}{F^4}+8C_{14}\frac{2m_K^4-2m_K^2m_\pi^2+m_\pi^4}{F^2} \\ +8C_{17}\frac{m_\pi^2(2m_K^2-m_\pi^2)}{F^2}+\frac{3A_0(m_\pi^2)}{128\pi^2F^2}+\frac{3A_0(m_K^2)}{64\pi^2F^2}+\frac{3c_\theta^2A_0(m_\eta^2)}{128\pi^2F^2}+\frac{3s_\theta^2A_0(m_{\eta'}^2)}{128\pi^2F^2}\Bigg]. \quad (2.32)$$

On the other hand, expressing the NLO and NNLO contributions in terms of F_π yields

$$F_K = F\Bigg[1+4L_5\frac{m_K^2}{F_\pi^2}+4L_4\frac{m_\pi^2+2m_K^2}{F_\pi^2}+8L_5^2\frac{3m_K^4+4m_K^2m_\pi^2}{F_\pi^4}-64L_5L_8\frac{m_K^4}{F_\pi^4} \\ +8C_{14}\frac{2m_K^4-2m_K^2m_\pi^2+m_\pi^4}{F_\pi^2}+8C_{17}\frac{m_\pi^2(2m_K^2-m_\pi^2)}{F_\pi^2} \\ +\frac{3A_0(m_\pi^2)}{128\pi^2F_\pi^2}+\frac{3A_0(m_K^2)}{64\pi^2F_\pi^2}+\frac{3c_\theta^2A_0(m_\eta^2)}{128\pi^2F_\pi^2}+\frac{3s_\theta^2A_0(m_{\eta'}^2)}{128\pi^2F_\pi^2}\Bigg]. \quad (2.33)$$

The expanded expression for the ratio of F_K/F_π in terms of F up to NNLO in δ expansion, takes the form

$$\frac{F_K}{F_\pi} = 1+4L_5\frac{m_K^2-m_\pi^2}{F^2}+8L_5^2\frac{3m_K^4-2m_K^2m_\pi^2-m_\pi^4}{F^4}+64L_5L_8\frac{m_\pi^4-m_K^4}{F^4} \\ +16C_{14}\frac{m_K^4-m_K^2m_\pi^2}{F^2}+16C_{17}\frac{m_K^2m_\pi^2-m_\pi^4}{F^2} \\ -\frac{5A_0(m_\pi^2)}{128\pi^2F^2}+\frac{A_0(m_K^2)}{64\pi^2F^2}+\frac{3c_\theta^2A_0(m_\eta^2)}{128\pi^2F^2}+\frac{3s_\theta^2A_0(m_{\eta'}^2)}{128\pi^2F^2}\,. \quad (2.34)$$

When expressing the previous result in terms of F_π, it reads

$$\frac{F_K}{F_\pi} = 1+4L_5\frac{m_K^2-m_\pi^2}{F_\pi^2}+8L_5^2\frac{3m_K^4+2m_K^2m_\pi^2-5m_\pi^4}{F_\pi^4}+64L_5L_8\frac{m_\pi^4-m_K^4}{F_\pi^4} \\ +16C_{14}\frac{m_K^4-m_K^2m_\pi^2}{F_\pi^2}+16C_{17}\frac{m_K^2m_\pi^2-m_\pi^4}{F_\pi^2} \\ -\frac{5A_0(m_\pi^2)}{128\pi^2F_\pi^2}+\frac{A_0(m_K^2)}{64\pi^2F_\pi^2}+\frac{3c_\theta^2A_0(m_\eta^2)}{128\pi^2F_\pi^2}+\frac{3s_\theta^2A_0(m_{\eta'}^2)}{128\pi^2F_\pi^2}\,, \quad (2.35)$$

which differs from eq. (2.34) in the L_5^2 term.

The pion squared mass up to NNLO is given by

$$m_\pi^2 = \overline{m}_\pi^2 + m_\pi^{2,\mathrm{NLO}} + m_\pi^{2,\mathrm{NNLO}}\,, \quad (2.36)$$

JHEP06(2015)175

with

$$\overline{m}_\pi^2 = 2B\widehat{m}\,, \tag{2.37}$$

$$m_\pi^{2,\mathrm{NLO}} = \frac{8(2L_8-L_5)m_\pi^4}{F^2}\,, \tag{2.38}$$

$$\begin{aligned} m_\pi^{2,\mathrm{NNLO}} = {} & \frac{8(2L_6-L_4)m_\pi^2(2m_K^2+m_\pi^2)}{F^2} - \frac{64(L_5^2-6L_5L_8+8L_8^2)m_\pi^6}{F^4} \\ & - \frac{16(2C_{12}+C_{14}+C_{17}-3C_{19}-2C_{31})m_\pi^6}{F^2} + \frac{m_\pi^2(c_\theta^2-2\sqrt{2}c_\theta s_\theta+2s_\theta^2)A_0(m_\eta^2)}{96\pi^2F^2} \\ & + \frac{m_\pi^2(2c_\theta^2+2\sqrt{2}c_\theta s_\theta+s_\theta^2)A_0(m_{\eta'}^2)}{96\pi^2F^2} - \frac{m_\pi^2A_0(m_\pi^2)}{32\pi^2F^2}\,. \end{aligned} \tag{2.39}$$

When expressing the renormalized m_π in terms of F_π, the only differences are the L_5L_8 and L_5^2 terms in eq. (2.39) and the other parts are the same as in eq. (2.36) with the explicit replacement of F by F_π in eq. (2.27). Therefore we only give the different parts for simplicity when expressing in terms of F_π and they read

$$m_\pi^{2,(F_\pi),\,L_5L_8\,,L_5^2} = \frac{128(4L_5L_8-L_5^2)m_\pi^6}{F_\pi^4}\,. \tag{2.40}$$

The mass squared for kaon up to NNLO is provided by

$$m_K^2 = \overline{m}_K^2 + m_K^{2,\mathrm{NLO}} + m_K^{2,\mathrm{NNLO}} \tag{2.41}$$

with

$$\overline{m}_K^2 = B(\widehat{m}+m_s)\,, \tag{2.42}$$

$$m_K^{2,\mathrm{NLO}} = \frac{8(2L_8-L_5)m_K^4}{F^2}\,, \tag{2.43}$$

$$\begin{aligned} m_K^{2,\mathrm{NLO}} = {} & \frac{8(2L_6-L_4)m_K^2(2m_K^2+m_\pi^2)}{F^2} - \frac{64(L_5^2-6L_5L_8+8L_8^2)m_K^6}{F^4} \\ & - \frac{32C_{12}m_K^6}{F^4} + \frac{32C_{31}m_K^6}{F^2} + \frac{16C_{17}m_K^2m_\pi^2(-2m_K^2+m_\pi^2)}{F^2} \\ & - \frac{16C_{14}m_K^2(2m_K^4-2m_K^2m_\pi^2+m_\pi^4)}{F^2} + \frac{48C_{19}m_K^2(2m_K^4-2m_K^2m_\pi^2+m_\pi^4)}{F^2} \\ & - \frac{[c_\theta^2(3m_\eta^2+m_\pi^2)+2\sqrt{2}c_\theta s_\theta(-2m_K^2+m_\pi^2)-4m_K^2s_\theta^2]A_0(m_\eta^2)}{192\pi^2F^2} \\ & - \frac{[-4c_\theta^2m_K^2+2\sqrt{2}c_\theta s_\theta(2m_K^2-m_\pi^2)+(3m_{\eta'}^2+m_\pi^2)s_\theta^2]A_0(m_{\eta'}^2)}{192\pi^2F^2}\,. \end{aligned} \tag{2.44}$$

When expressing eq. (2.41) in terms of F_π, the differences are the L_5L_8 and L_5^2 terms in eq. (2.44) and the new expressions are

$$m_K^{2,(F_\pi),\,L_5L_8\,,L_5^2} = -\frac{64L_5^2m_K^4(m_K^2+m_\pi^2)}{F_\pi^4} + \frac{128L_5L_8m_K^4(3m_K^2+m_\pi^2)}{F_\pi^4}\,. \tag{2.45}$$

Notice that the masses of pion and kaon appearing in NLO and NNLO parts in the above equations correspond to the renormalized quantities, instead of their LO expressions. In addition, this gives the quark mass ratio relation $m_s/\hat{m} = 2\overline{m}_K^2/\overline{m}_\pi^2 - 1$.

JHEP06(2015)175

When performing the chiral extrapolation of the lattice data, instead of the renormalized m_K^2 as in the previous equations, it is convenient to use the LO kaon mass squared in the higher order corrections. In this way, we do not need to iteratively solve eq. (2.41) in order to give the value of m_K for a given m_π. The result in terms of $\overline{m}_K$ in the NLO and NNLO expressions becomes

$$m_K^{2,\mathrm{Lat}} = \overline{m}_K^2 + m_K^{2,\mathrm{Lat-NLO}} + m_K^{2,\mathrm{Lat-NNLO}}\,, \tag{2.46}$$

with

$$m_K^{2,\mathrm{Lat-NLO}} = \frac{8(2L_8 - L_5)\overline{m}_K^4}{F^2}\,, \tag{2.47}$$

$$\begin{aligned} m_K^{2,\mathrm{Lat-NNLO}} = {} & \frac{8(2L_6-L_4)\overline{m}_K^2(2\overline{m}_K^2+m_\pi^2)}{F^2} + \frac{64(L_5^2-2L_5L_8)\overline{m}_K^6}{F^4} - \frac{32C_{12}\overline{m}_K^6}{F^4} + \frac{32C_{31}\overline{m}_K^6}{F^2} \\ & + \frac{16C_{17}\overline{m}_K^2 m_\pi^2(-2\overline{m}_K^2+m_\pi^2)}{F^2} - \frac{16C_{14}\overline{m}_K^2(2\overline{m}_K^4 - 2\overline{m}_K^2 m_\pi^2 + m_\pi^4)}{F^2} \\ & + \frac{48C_{19}\overline{m}_K^2(2\overline{m}_K^4 - 2\overline{m}_K^2 m_\pi^2 + m_\pi^4)}{F^2} \\ & - \frac{[c_\theta^2(3m_\eta^2+m_\pi^2) + 2\sqrt{2}c_\theta s_\theta(-2\overline{m}_K^2+m_\pi^2) - 4\overline{m}_K^2 s_\theta^2]A_0(m_\eta^2)}{192\pi^2F^2} \\ & - \frac{[-4c_\theta^2\overline{m}_K^2 + 2\sqrt{2}c_\theta s_\theta(2\overline{m}_K^2 - m_\pi^2) + (3m_{\eta'}^2 + m_\pi^2)s_\theta^2]A_0(m_{\eta'}^2)}{192\pi^2F^2}\,. \end{aligned} \tag{2.48}$$

When expressing eq. (2.46) in terms of F_π, the differences are the L_5L_8 and L_5^2 terms in eq. (2.48) and the new expressions are

$$m_K^{2,\mathrm{Lat},(F_\pi),\,L_5L_8\,,L_5^2} = \frac{64L_5(L_5-2L_8)\overline{m}_K^4(\overline{m}_K^2 - m_\pi^2)}{F_\pi^4}\,. \tag{2.49}$$

When confronting with the lattice data, we only consider the simulated points with the physical strange-quark mass, i.e. the lattice ensembles that when extrapolating to the physical pion masses lead simultaneously to physical kaon masses. In this case, we can express the LO kaon mass squared as

$$\overline{m}_K^2 = B(m_s^{\mathrm{Phy}} + \widehat{m}) = B(m_s^{\mathrm{Phy}} + \widehat{m}^{\mathrm{Phy}}) - B\widehat{m}^{\mathrm{Phy}} + B\widehat{m} = \overline{m}_K^{2,\mathrm{Phy}} - \frac{\overline{m}_\pi^{2,\mathrm{Phy}}}{2} + \frac{\overline{m}_\pi^2}{2}\,, \tag{2.50}$$

where $\overline{m}_K^{2,\mathrm{Phy}}$ and $\overline{m}_\pi^{2,\mathrm{Phy}}$ can be obtained through eqs. (2.36) and (2.41) by substituting the physical masses of π, K, η, η' in the NLO and NNLO expressions. For $\overline{m}_\pi^2$, which varies in the lattice simulation, we can extract its value by using eq. (2.36). In this case, m_π in eq. (2.36) takes the value from lattice simulation, and $m_K, m_\eta, m_{\eta'}$, which only appear in the NNLO part, can be approximated by their LO expressions.

In the above discussions, we have distinguished the situations of using $1/F^2$ and $1/F_\pi^2$ in the higher order corrections for various observables. Similarly, we can also generalize the discussions by replacing the renormalized masses (m_π and m_K) with the LO ones ($\overline{m}_\pi$ and $\overline{m}_K$) in the higher order corrections. We take the observables F_π and F_K as examples to illustrate the differences. The renormalized m_π and m_K have been used in eqs. (2.29)

JHEP06(2015)175

and (2.32) for F_π and F_K with $1/F^2$ in the higher order terms, respectively. After replacing m_π and m_K in eqs. (2.29) and (2.32) with their expressions in terms of the LO masses $\overline{m}_\pi$ and $\overline{m}_K$ through eqs. (2.36) and (2.41) respectively, the corresponding expressions are found to be

$$F_\pi = F\left[1+4L_5\frac{\overline{m}_\pi^2}{F^2}+4L_4\frac{\overline{m}_\pi^2+2\overline{m}_K^2}{F^2}-8L_5^2\frac{\overline{m}_\pi^4}{F^4}+(8C_{14}+8C_{17})\frac{\overline{m}_\pi^4}{F^2}+\frac{A_0(\overline{m}_\pi^2)}{16\pi^2F^2}+\frac{A_0(\overline{m}_K^2)}{32\pi^2F^2}\right], \tag{2.51}$$

$$\begin{aligned} F_K = F\Bigg[&1+4L_5\frac{\overline{m}_K^2}{F^2}+4L_4\frac{\overline{m}_\pi^2+2\overline{m}_K^2}{F^2}-8L_5^2\frac{\overline{m}_K^4}{F^4}+8C_{14}\frac{2\overline{m}_K^4-2\overline{m}_K^2\overline{m}_\pi^2+\overline{m}_\pi^4}{F^2} \\ &+8C_{17}\frac{\overline{m}_\pi^2(2\overline{m}_K^2-\overline{m}_\pi^2)}{F^2}+\frac{3A_0(\overline{m}_\pi^2)}{128\pi^2F^2}+\frac{3A_0(\overline{m}_K^2)}{64\pi^2F^2}+\frac{3c_\theta^2A_0(\overline{m}_\eta^2)}{128\pi^2F^2}+\frac{3s_\theta^2A_0(\overline{m}_{\eta'}^2)}{128\pi^2F^2}\Bigg]. \end{aligned} \tag{2.52}$$

As in the discussion of $1/F^2$ versus $1/F_\pi^2$ up to the NNLO precision, the expressions for a specific observable by using the renormalized masses m_π, m_K and the LO $\overline{m}_\pi, \overline{m}_K$ only differ in the terms like L_iL_j, being L_i and L_j the NLO LECs in eq. (2.4). This can be clearly seen when comparing eqs. (2.29) and (2.51). E.g. the differences caused by using the renormalized masses and the LO ones are the L_5^2 and L_5L_8 terms, apart from the explicit replacement of m_π and m_K by $\overline{m}_\pi$ and $\overline{m}_K$ respectively. Similar rules are also applied to eqs. (2.32) and (2.52).

To replace m_π, m_K by $\overline{m}_\pi$ and $\overline{m}_K$ in the NLO and NNLO corrections in eq. (2.36), the only changes happen for the L_iL_j terms and the corresponding new expressions read

$$m_\pi^{2,(\overline{m}_\pi,\overline{m}_K,F),\,L_5L_8\,,L_5^2\,,L_8^2} = \frac{64L_5(L_5-2L_8)\overline{m}_\pi^6}{F^4}\,. \tag{2.53}$$

In principle, we should also present the results expressed with the LO masses $\overline{m}_\pi, \overline{m}_K$ and the renormalized decay constants F_π, F_K, which can be straightforwardly obtained by substituting the relations in eqs. (2.36) and (2.41) into the corresponding observables. We consider the expressions given in terms of the renormalized masses and $1/F^2$ as our preferred ones in this work. The reason to choose the renormalized masses is for practical purpose, since in lattice simulations the different observables are typically given as functions of the renormalized m_π^2. Also most of the chiral studies choose to express the quantities with the renormalized masses in the higher order corrections, such as in refs. [52, 53]. Following this rule we consider the results with the renormalized masses and $1/F_\pi^2$ as an estimate of systematic errors due to the truncation of the δ expansion when one works at a given order in perturbation theory. While for the case with the LO masses, we shall also comment the results in the following numerical discussions.

3 Phenomenological discussions

The big challenge in the present general discussions on the η-η' mixing is the determination of the unknown LECs in eqs. (2.1), (2.4) and (2.5). The recent lattice simulations on the light pseudoscalar mesons provide us valuable sources to constrain these free parameters. The considered lattice simulations include the m_π dependences of the masses of η, η' [15–19]

JHEP06(2015)175

and kaon [22, 23], and the π, K decay constants [22, 23] and their ratios [24]. Moreover, relevant phenomenological results and experimental data will be also included to constrain the LECs.

Since we do not consider the isospin violating effects, we will take the values for the physical pion and kaon masses in the isospin limit from ref. [54], where the corrections from the electromagnetic contributions are removed,

$$m_\pi = 135.0 \text{ MeV}\,, \qquad m_K = 494.2 \text{ MeV}\,. \tag{3.1}$$

These values will be used in later chiral extrapolations, while for the physical masses of η and η' and the decay constants of pion and kaon, we will take their world-average values from ref. [55].

In order to show the results step by step, we present the discussions in the following sections split in three parts: we consider fits performed at leading order, next-to-leading order and next-to-next-to-leading order.

3.1 Leading-order analyses

At leading order, the η-η' mixing is described by one free parameter, namely the singlet η_0 mass M_0 in eq. (2.1) and the explicit expressions for the masses and mixing angle are given in eqs. (2.8), (2.9) and (2.10). At this order, the π, K decay constants are degenerate and given by their chiral and large N_C limits, i.e. $F_\pi = F_K = F$. Therefore we shall not take the lattice simulations of the decay constants into account for the LO discussion as they clearly show the need of higher order corrections for a suitable description. Also at leading order, F will not enter the masses and mixing angle, as shown in eqs. (2.8), (2.9) and (2.10). As a result of this, we do not need to distinguish the two situations with F or F_π discussed previously in the expressions of different observables. Apart from the lattice simulation data, we also fit the physical values of the η and η' masses. Nonetheless, fitting the physical masses with the experimental precision at the level of several hundred-thousandth is too ambitious. Since the ultimate goal of the present work is the NNLO study, the ballpark estimate of our theoretical uncertainty, starting from the N^{3}LO part, should be around 3%. This value is obtained from the general rule that each higher order correction in δ expansion, either the SU(3)-flavor breaking or the $1/N_C$ effect, is around 30%. In fact, the estimated three-percent uncertainty is also similar to the typical error bars reported in many lattice simulations, in the range from $3-10\%$ [15–19]. Consistently, we assign a 1% uncertainty to the physical values of m_η and $m_{\eta'}$ in the fits.

The value of the singlet mass M_0 from the LO fit is

$$M_0 = (835.7 \pm 7.5)\,\text{MeV}\,. \tag{3.2}$$

The physical masses for the η, η' and their LO mixing angle θ from the fit are found to be

$$m_\eta = (496.4 \pm 1.3)\,\text{MeV}\,, \quad m_{\eta'} = (969.8 \pm 5.8)\,\text{MeV}\,, \theta = -18.9^\circ \pm 0.3^\circ\,. \tag{3.3}$$

The resulting plots can be seen in figure 1. We verify that if the physical masses are excluded in the fit, $M_0 = 813 \pm 11\,\text{MeV}$ results. If we only include the physical masses

JHEP06(2015)175

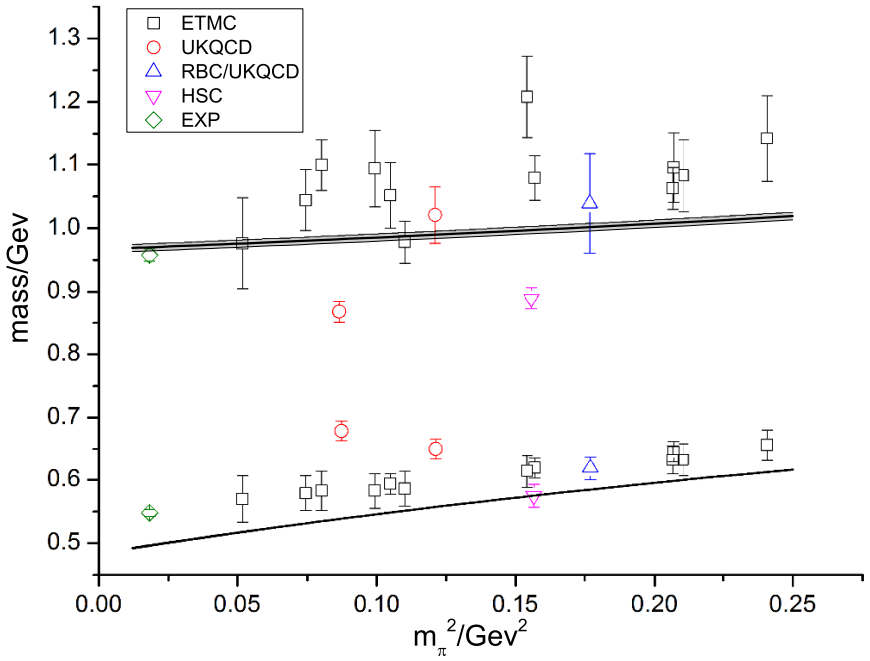

Figure 1. The masses of η and η' from the LO fit. The left most two points correspond to the physical masses. The remaining lattice simulation data are taken from refs. [18, 19] (ETMC), [17] (UKQCD), [16] (RBC/UKQCD), [15] (HSC), where we only take into account the simulation points with $m_\pi < 500\,\text{MeV}$. The shade area surrounding each curve stands for the statistical uncertainty from the fit.

and exclude the lattice simulation data in the fit, $M_0 = 859 \pm 11\,\text{MeV}$ is obtained. These determinations of M_0 lie within the broad range summarized in ref. [51] and are quite close with the commonly used values of $M_0 = 850\,\text{MeV}$ [51]. Taking into account the large uncertainties of the lattice simulation data, specially for $m_{\eta'}$, and the concise formalism of the LO mixing, it is impressive that the lattice simulation data can already be qualitatively described with the LO analysis, as shown in figure 1. This also indicates that the higher order mixing effects can only give moderate corrections to the masses of η and η'.

Nevertheless, in order to describe the lattice data more accurately, specially the η masses, the chiral corrections beyond the leading order are needed. For the physical masses, it has also been shown that the LO description fails to explain the mass ratio of η and η' accurately enough [49]. Therefore it is essential to generalize the discussions to NLO and NNLO in order to achieve a precise description both for lattice simulations and physical data.

3.2 Next-to-leading order analyses

At next-to-leading order, in addition to the parameter M_0 at leading order, there are five additional free parameters: the decay constant F at chiral and large N_C limits, and the four NLO LECs L_5, L_8, Λ_1 and Λ_2 in eq. (2.4). At this order, as well as at next-to-

JHEP06(2015)175

next-to-leading order, one can rewrite the chiral expansion of the observables in various equivalent ways up to the perturbative order in δ under consideration. In the following discussion, we will perform two types of fits: one using F in the theoretical NLO and NNLO expressions and the other employing F_π, as discussed in section 2.4. Since the differences of the theoretical expressions used in the two types of fits are beyond the considered precision, the variances of the outputs from the two fits can be considered as systematic errors from the theoretical models by neglecting higher order contributions. In the following, we will explicitly present the fit results by using F in the theoretical expressions, which is the most straightforward option, as discussed in section 2.4. The outputs of the fits with the theoretical formulas expressed in terms of F_π will be used to estimate the systematic errors: the difference between the central values of the two types of fits will be used to estimate the truncation uncertainty due to working just up to a given order in the δ-expansion, providing the second error for each quantity in the following tables.

In refs. [42–44], it is argued that at each chiral order, the leading N_C effects are dominant, or in other words that the Λ_1 and Λ_2 terms are assumed to be much less irrelevant than the L_5 and L_8 terms in the NLO δ expansion. This assumption has been more or less confirmed when focusing on the masses of η, η' and the LO mixing angle at the physical points [42–44]. In ref. [45], the local higher order LECs were estimated by the tree-level resonance exchanges and it was found that with those LECs Λ_2 seems to be more important than Λ_1 when focusing on the physical masses for η and η'. It is interesting to check how these assumptions work when including the lattice simulations and the phenomenological results of the two-mixing-angle parameters, which are not considered in refs. [42–45]. Different sets of fits to the lattice data and phenomenological inputs from the two-mixing-angle scheme are performed either by fixing $\Lambda_{i=1,2}$ to zero or releasing their values, in order to reexamine the assumptions. Interestingly we do not find qualitative changes between the fits with fixed $\Lambda_{i=1,2} = 0$ and the ones with free values for these parameters. This tells us that indeed the Λ_1 and Λ_2 terms do not significantly improve the fit results, even after taking into account the lattice simulations. Nevertheless, we find that these two terms are quite important to reproduce the phenomenological mixing angles θ_0 and θ_8 in the fits where M_0 is fixed at its LO value. If M_0 is released in the fits we find that including Λ_1 and Λ_2 improves the descriptions of $m_{\eta'}$ from lattice simulations. Therefore, we will not further discuss fits with Λ_1 and Λ_2 set to zero in the following. Instead, we focus on the results given in table 1 with all the four NLO LECs in the fits, namely L_5, L_8, Λ_1 and Λ_2 in eq. (2.4).

For the parameter M_0, we take two strategies to estimate its value in NLO analysis. In one of them we fix $M_0 = 835.7\,\text{MeV}$ from its LO determination (NLOFit-A) and in the other case we free its value for the NLO fit (NLOFit-B). These two NLO fits are given in table 1. The first error bar for each fitted parameter corresponds to the statistical one from the fits and the second error bar is estimated from the variation of the fits between those using F and F_π in the NLO (and later also NNLO) theoretical expressions. From the two fits shown in table 1, one can see that releasing M_0 in the fits barely changes the fit quality with respect to the cases when its value is fixed, although there are slight variations in the determinations of M_0 and Λ_2.

JHEP06(2015)175

Concerning the results of the LECs in table 1, the resulting values for F from the two fits are quite compatible and close to the physical pion decay constant. For Λ_1 and Λ_2, their values are poorly known in literature and it is helpful to compare our values with the following estimate for their ranges: we take the LO determination $M_0 = 835.7\,\text{MeV}$, and we then separately include the Λ_1 and Λ_2 terms in the η-η' mixing and vary their values to obtain new results for m_η and $m_{\eta'}$ with the physical m_π. Since the Λ_1 and Λ_2 terms are NLO $1/N_C$ effects, it is reasonable to assume that their corrections to m_η^2 or $m_{\eta'}^2$ should be at most around 30% of the LO results. In this way we can set up conservative and rough estimates for the ranges of Λ_1 and Λ_2, which are found to be

$$|\Lambda_1| < 0.4\,, \qquad |\Lambda_2| < 0.7\ . \tag{3.4}$$

The resulting magnitudes of Λ_1 in our fits are tiny and consistent with zero, as shown in table 1. For the parameter Λ_2, our determinations lie within the ranges estimated in eq. (3.4). Its value, specially the one from NLOFit-A, is close to the one used in ref. [56], where the mixing was discussed at next-to-leading order. However the determinations for Λ_2 in table 1 become much more precise than those given in refs. [45, 47], where the lattice simulations for m_η and $m_{\eta'}$ are not included, indicating the usefulness of incorporating the lattice data in the U(3) χPT study. Our determinations of L_5 and L_8 are in good agreement with the leading N_C predictions from resonance chiral theory [57], the SU(3) one-loop results in refs. [1, 2] and the one-loop resonance chiral theory determination for L_8 [58, 59]. But the values here are clearly larger than those from the recent two-loop determinations [26, 27], the results from $K\pi$ scattering in the scalar channels [60], and the one-loop resonance chiral theory estimates for L_5 [29]. The discrepancies of L_5 and L_8, comparing with the recent two-loop determinations [26, 27], can be eliminated once the $\mathcal{O}(p^6)$ LECs are taken into account, as we will show in the NNLO discussion.

The values of the parameters in the two-mixing-angle scheme and the mass ratio of strange and up/down quarks resulting from the fits are given in table 2. Similarly, the first error bar for each quantity is the statistical error and the second one corresponds to the systematic error, which is obtained in the same way as the one in table 1. Notice that these inputs have already been satisfactorily reproduced in NLO analyses.

The other quantities in the fits are presented in figures 2, 3, 4 and 5, together with the lattice simulation data and the experimental inputs. We find that the final outputs from NLOFit-A and NLOFit-B are quite similar, so only the plots from NLOFit-B are given explicitly. The shaded area surrounding each curve corresponds to the statistical error band for each quantity. In figure 2, we show the resulting figures from NLOFit-B for the masses of η and η'. In figures 3, 4 and 5, we show the corresponding plots for m_K^2, $F_{\pi,K}$ and F_K/F_π as functions of m_π^2, respectively.

3.3 NLO fits focusing on the masses

In this section, we present another kind of NLO fits by focusing on the masses of η, η', K and excluding the decay constants F_π, F_K and their ratio. This kind of discussion is well motivated, since it is known that the NNLO corrections in δ counting, such as the LEC

JHEP06(2015)175

	NLOFit-A	NLOFit-B
$\chi^2/(d.o.f)$	481.2/(76-5)	477.7/(76-6)
M_0 (MeV)	835.7*	767.3±31.5±32.3
F (MeV)	92.1±0.2±0.6	92.1±0.2±0.6
$10^3 \times L_5$	1.45±0.02±0.30	1.47±0.02±0.29
$10^3 \times L_8$	1.00±0.07±0.10	1.08±0.05±0.04
Λ_1	0.02±0.05±0.06	-0.09±0.08±0.02
Λ_2	0.25±0.06±0.02	0.14±0.07±0.03

Table 1. Parameters from the NLO fits. The meaning of different notations to label different fits are explained in detail in the text. In the row of M_0, the columns with 835.7* denote the fit results by fixing the value of M_0 from its LO determination. The first error bar for each parameter is the statistical one given by the fits and the second one corresponds to the systematic error. The way to estimate the systematic error is explained in detail in the text.

Parameters	Inputs	NLOFit-A	NLOFit-B
F_0 (MeV)	118.0 ±16.5	104.9±2.9±0.3	99.7±3.6±1.6
F_8 (MeV)	133.7 ±11.1	113.2±0.3±4.4	113.5±0.3±4.2
θ_0 (Degree)	-11.0 ±3.0	-7.2±2.1±1.3	-10.6±2.4±0.1
θ_8 (Degree)	-26.7 ±5.4	-21.5±2.2±3.9	-25.4±2.6±2.3
$m_s/\widehat{m}$	27.5 ±3.0	22.6±0.8±0.6	21.9±0.6±1.2
F_q (MeV)	106.0 ± 11.1*	94.1±1.9±1.7	90.6±2.4±0.4
F_s (MeV)	143.8 ± 16.5*	122.3±1.2±5.1	120.9±1.2±5.5
θ_q (Degree)	34.5 ± 5.4*	40.4±3.1±3.6	35.0±3.7±1.6
θ_s (Degree	36.0 ± 4.2*	39.9±1.7±2.2	37.2±1.8±1.1

Table 2. The outputs from NLO fits. Notice that F_q, F_s, θ_q and θ_s are not the phenomenological inputs in the fits, since they are related to F_0, F_8, θ_0 and θ_8 through eq. (2.24). The phenomenological values for the mixing parameters are taken from ref. [21] and we triple the error bands here in order to make a conservative estimate. The input of $m_s/\widehat{m}$ is taken from the FLAG working group in ref. [54] and we assign the 10% error bar as done in ref. [26]. For the error bars of each quantity, the first one corresponds to the statistic error and the second one is for the systematic error, which are explained in detail in the text.

L_4, are important to simultaneously describe F_π and F_K [26–28]. But this LEC is absent in NLO study. We have also provided another independent confirmation on this finding in figure 4, where one can see that the decay constants of pion and kaon are poorly reproduced at next-to-leading order in δ expansion. When only focusing on the η, η' and K masses and the ratio $m_s/\hat{m}$ at next-to-leading order the parameter F can not be resolved, because it always appears in the form L_5/F^2 or L_8/F^2. We will fix its value to $F = 90\,\mathrm{MeV}$, close to the values given in table 1. For the mixing parameters we consider the mixing angles of θ_0 and θ_8, but exclude the constants F_0 and F_8. This is because F_0 and F_8 are dependent on the parameter F and should be determined together with F_π and F_K. For simplicity in later discussion, we call the fits performed in this section as the mass-focusing type throughout.

JHEP06(2015)175

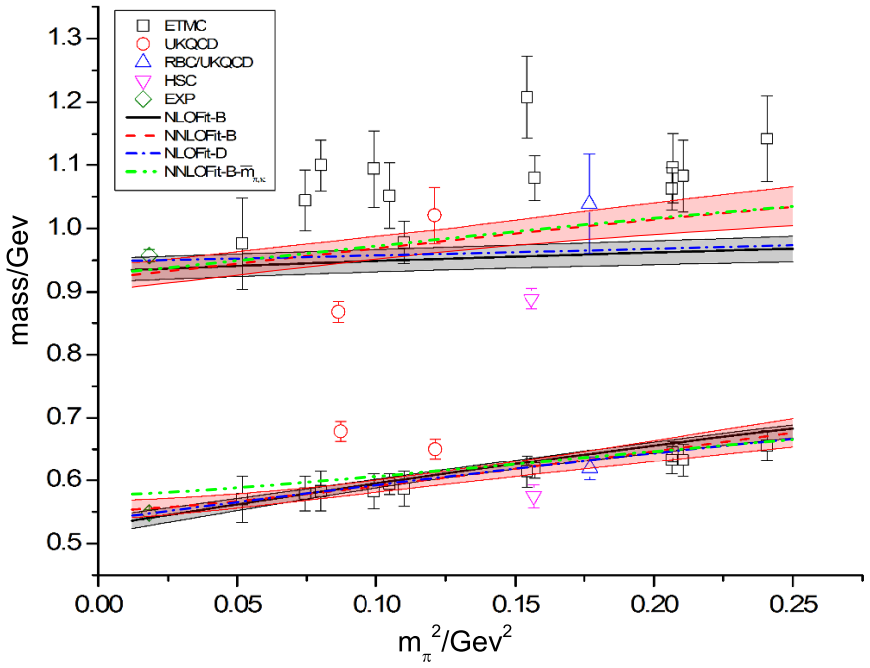

Figure 2. The masses of η and η' from the NLO and NNLO fits. The left most two points correspond to the physical masses. The remaining lattice simulation data are taken from refs. [18, 19] (ETMC), [17] (UKQCD), [16] (RBC-UKQCD), [15] (HSC), where we only take into account the points with $m_\pi < 500\,\text{MeV}$. The shaded areas around the black solid and red dashed lines stand for the statistical error bands from the NLOFit-B and NNLOFit-B fits, respectively. The meaning of notations for different lines are explained in detail in the text.

As in the previous section, we present the fits with F in the denominators of the theoretical expressions (e.g. eq. (2.27)) and use the fits with F_π to estimate the systematic errors. For each case, we perform the fits either by fixing M_0 at its LO determination (NLOFit-C) or by freeing its value (NLOFit-D). The fitted parameters are given in table 3 and the $m_s/\hat{m}$ ratio and mixing angles are given in table 4. The resulting figures from NLOFit-C and NLOFit-D are quite similar and we explicitly show one set of them, e.g. NLOFit-D in figures 2 and 3 for the $\eta^{(\prime)}$ and kaon masses, respectively.

A significant difference between the results in table 1 and the mass-focusing fits in table 3 is that much larger statistical error bars are obtained in the latter case, especially for the LECs L_5 and L_8, as they are constrained by fewer data. Likewise, there are large systematic errors for the values of L_5 and L_8 in table 3, indicating a larger truncation uncertainty due to higher orders. We do not see a significant improvement when freeing the value of M_0 in the fits.

3.4 Next-to-next-to-leading order analyses

From the NLO discussions in the previous two sections, we observe that the phenomenological results and the lattice simulations on η and η' states can be reasonably reproduced.

JHEP06(2015)175

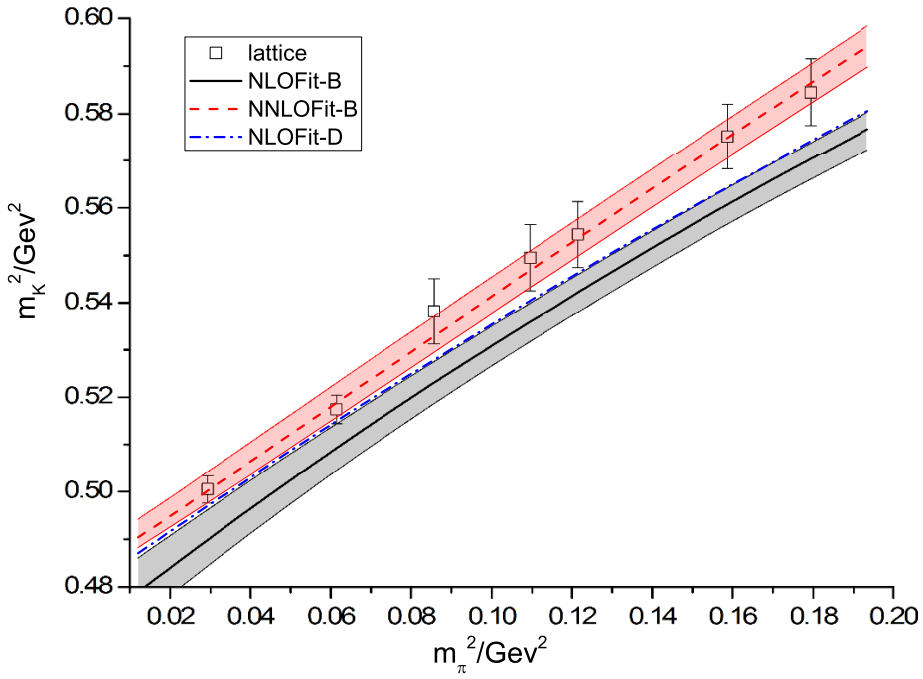

Figure 3. Kaon mass from the NLO and NNLO fits. The lattice simulation data are taken from RBC and UKQCD [22, 23]. Only the unitary points simulated with the physical strange quark mass are included. The shaded areas around the black solid and red dashed lines stand for the statistical error bands from the NLOFit-B and NNLOFit-B fits, respectively. The meaning of notations for different lines are explained in detail in the text.

	NLOFit-C	NLOFit-D
$\chi^2/(d.o.f)$	168.8/(44-4)	168.7/(44-5)
M_0 (MeV)	835.7*	821.5±43.5
$10^3 \times L_5$	1.40±0.58±0.75	1.51±0.68±0.91
$10^3 \times L_8$	0.88±0.29±0.35	0.94±0.34±0.44
Λ_1	-0.06±0.04±0.02	-0.09±0.11±0.09
Λ_2	0.17±0.19±0.25	0.18±0.19±0.25

Table 3. Parameters from the mass-focusing NLO fits. The meaning of different notations to label different fits are explained in detail in the text. F is fixed at 90 MeV in these fits. The first error for each parameter corresponds to the statistical one and the second error denotes the systematic uncertainty. See the text for details.

JHEP06(2015)175

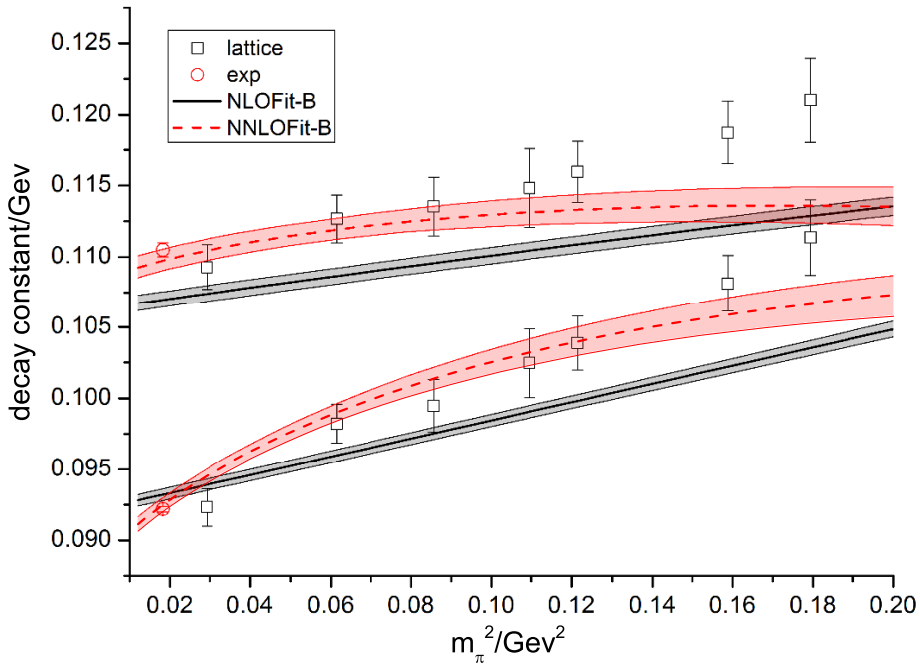

Figure 4. Pion and kaon decay constants from the NLO and NNLO fits. The left-most points for F_π and F_K correspond to the physical experimental inputs. The remaining lattice simulation data are taken from RBC and UKQCD [22, 23], where we have only included the unitary points simulated with the physical strange quark mass. The shaded area around each curve stands for the statistical error band from the fits. The meaning of notations for different lines are explained in detail in the text.

Parameters	Inputs	NLOFit-C	NLOFit-D
θ_0 (Degree)	-11.0 ±3.0	-10.6±2.4±3.3	-11.0±3.4±2.1
θ_8 (Degree)	-26.7 ±5.4	-25.3±2.4±4.4	-26.7±4.5±7.1
$m_s/\widehat{m}$	27.5 ±3.0	23.7±0.3±0.3	23.6±0.5±0.1
θ_q (Degree)	34.5 ± 5.4*	35.6±1.4±1.1	34.1±4.3±4.1
θ_s (Degree)	36.0 ± 4.2*	37.0±0.9±0.7	36.3±2.2±2.1

Table 4. The outputs from the mass-focusing NLO fits. See table 2 for the phenomenological inputs. The first error for each quantity corresponds to the statistical one and the second error denotes the systematic uncertainty. See the text for details.

JHEP06(2015)175

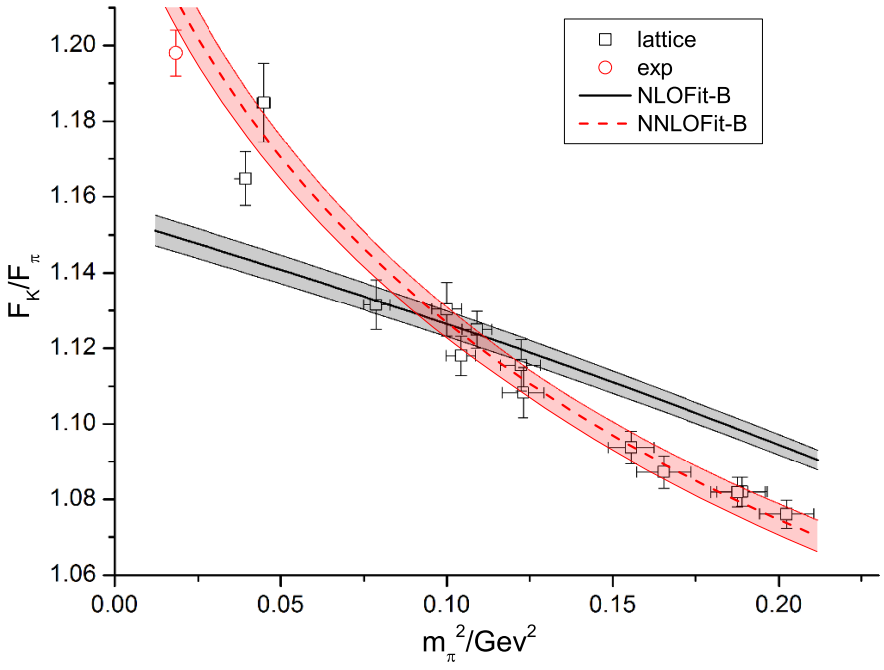

Figure 5. Ratio F_K/F_π from the NLO and NNLO fits. The left most point corresponds to the experimental input. The remaining lattice simulation data are taken from ref. [24] (BMW). The shaded area around each curve stands for the statistical error band from the fits. The meaning of notations for different lines are explained in detail in the text.

This is an important improvement comparing with the LO study, since at this order we only have the conventional one-mixing-angle formalism. The two-mixing-angle formalism only shows up beyond LO. However, observing m_K, F_π, F_K and their ratio in figures 3, 4 and 5, it is clear that the NLO analysis is still inadequate. We need to include higher order contributions beyond NLO in order to further improve the descriptions. Moreover, the chiral logarithms predicted by χPT at one loop start at NNLO in the δ expansion. Due to their importance in other observables, we consider it is relevant to discuss the impact of these chiral logs.

As in the NLO case, we perform two types of fits, using the NLO and NNLO theoretical expressions given in terms of F and F_π for various observables. We explicitly present the fit results with F in the theoretical expressions and use the alternative fits expressed in terms of F_π to estimate the systematic errors, due to working up to NNLO in δ and neglecting higher orders. According to the Lagrangian in eq. (2.5), eleven additional unknown LECs appear at NNLO and there will be seventeen parameters in total for the NNLO study. At the present precision of the lattice simulations and phenomenological inputs, it is impossible to obtain sensible and stable fits if we free all of the seventeen parameters. Therefore, we need to take other independent determinations for some of the LECs in order to proceed the NNLO study.

JHEP06(2015)175

We mention that the state-of-art determinations of the $\mathcal{O}(p^4)$ LECs in SU(3) χPT suffer uncertainties from the many poorly known $\mathcal{O}(p^6)$ LECs [26, 27]. Because of the large number of barely known $\mathcal{O}(p^6)$ LECs, it is rather difficult to get conclusive results in the present two-loop SU(3) χPT studies [26, 27]. In the present work, there are five $\mathcal{O}(p^6)$ LECs, i.e. $C_{12}, C_{14}, C_{17}, C_{19}, C_{31}$, in eq. (2.5) and we cannot make precise determinations of these C_i parameters here. Maybe when taking into account the scattering data, one can make more stringent constraints on the C_i LECs in U(3) χPT. But this is beyond the scope of current work. Instead we take the C_i values from the Dyson-Schwinger-like approach given in ref. [61], where all of the $\mathcal{O}(p^6)$ C_i at leading N_C are predicted. In order to show the dependences of the final results on the C_i values, we also perform other fits by using their updated determinations [62]. Like in ref. [26], we multiply the $\mathcal{O}(p^6)$ C_i from refs. [61, 62] by a global factor α and consider α as a free parameter in the fits. In this way, we partially compensate the large uncertainties of the C_i parameters.

For the operators proportional to $v_2^{(2)}$, L_{18} and L_{25} in eq. (2.5), they are not present in SU(3) χPT and purely contribute to the η-η' mixing, being irrelevant to the pion and kaon observables. Since the η-η' mixing parameters have already been satisfactorily described in the NLO fits, we do not further include $v_2^{(2)}$, L_{18} and L_{25} at NNLO study.[2] Their inclusion in the present analysis tend to make the fit unstable. Clearly studying more $\eta^{(\prime)}$ related observables it would be possible to extract these parameters but this is out of the reach of the present analysis. A global fit is too unconstrained, being unstable and producing values of the latter couplings compatible with zero within uncertainties. Then we are left with three $\mathcal{O}(N_C^0, p^4)$ operators: L_4, L_6 and L_7, which have corresponding parts in SU(3) χPT. Since U(3) and SU(3) χPT contain different dynamical degrees of freedom, the corresponding LECs from the two theories can be different. A typical example is the L_7 parameter in SU(3) χPT, which is demonstrated to be dominated by the singlet η_0 state [1, 2]. Since in U(3) χPT the singlet η_0 has been explicitly introduced, the value of L_7 in this theory can be totally different from $L_7^{\mathrm{SU(3)}}$ in SU(3) case. While for other $\mathcal{O}(p^4)$ LECs, such as $L_{i=4,5,6,8}$, the differences between U(3) and SU(3) χPT are not expected to be as large as the L_7 case, since they do not receive the tree-level contributions from the η_0 state.

Another subtlety to take into account is that m_η and $m_{\eta'}$ appear in the chiral loops and, at the same time, the final expressions of m_η and $m_{\eta'}$ depend on the these loops as well. In order to avoid making the complicated iterative procedure to obtain the η-η' mixing parameters, we use the LO formulas for m_η and $m_{\eta'}$ in the chiral loops. The differences caused by this simple treatment and the strict iterative procedure are beyond the NNLO precision in δ expansion, since the chiral loops themselves are already NNLO. Our simple solution is also justified by the fact that the LO description of m_η and $m_{\eta'}$ is in qualitative agreement with the lattice simulation data, as shown in section 3.1. Since the

[2]Indeed, in this work M_0 and $v_2^{(2)}$ only enter in the mass Lagrangian in eq. (2.14) explicitly. They always appear combined in the effective form $M_{0,\,eff}^2 = M_0^2 + 6v_2^{(2)}(2m_K^2 + m_\pi^2)$, which is the parameter we are actually extracting. The contribution $v_2^{(2)}$ could be singled out through the study of the $\eta_0\eta_0 \to \pi\pi$ scattering. However we point out that the anti-correlation between M_0 and $v_2^{(2)}$ in general can not be recovered in the present numerical fits, due to the presence of far too many parameters in the problem and the large uncertainties of the lattice simulation data, specially for the determinations of $m_{\eta'}$.

JHEP06(2015)175

qualitative agreement between the LO formulas and the lattice simulation data requires the value of M_0 to be around 835.7 MeV, as given in eq. (3.2), we fix $M_0 = 835.7\,\mathrm{MeV}$ in the following discussions. This also helps to stabilize the NNLO fits, with its many free parameters. Other useful criteria to discriminate reasonable fits are the a priori ranges estimated in eq. (3.4), since the fits with large magnitudes of Λ_1 and Λ_2 imply unphysically large corrections to the η-η' mixing parameters and the breakdown of the δ expansion. In the following we only present the fit results that are consistent with eq. (3.4).

With all of the above setups, the values of parameters from the NNLO fits are summarized in table 5. The fits labeled by NNLOFit-A and NNLOFit-B correspond to using different values of the $\mathcal{O}(p^6)$ LECs. For NNLOFit-A, the C_i values are taken from ref. [61]:

$$C_{12} = -0.34\,, \quad C_{14} = -0.83\,, \quad C_{17} = 0.01\,, \quad C_{19} = -0.48\,, \quad C_{31} = -0.63\,, \tag{3.5}$$

which are given in units of $10^{-3}\mathrm{GeV}^{-2}$. For NNLOFit-B, we take their updated $\mathcal{O}(p^6)$ C_i values from ref. [62]:

$$C_{12} = -0.34\,, \quad C_{14} = -0.87\,, \quad C_{17} = 0.17\,, \quad C_{19} = -0.27\,, \quad C_{31} = -0.46\,, \tag{3.6}$$

in the same units as before.

It is clear that the parameters resulting from fits with different C_i inputs slightly differ from one another. We remind that the first error bar for each parameter in table 5 corresponds to the statistical one directly from the fits and the second error bar stands for the systematic one, which is estimated, as usual, from the variation of the parameter from the NNLO fits with the theoretical expressions in terms of F and those expressed as functions of F_π.

At NNLO, one has the contributions from the chiral loops and the $\mathcal{O}(p^6)$ LECs, which make our determinations in table 5 closer to the recent two-loop results of the SU(3) χPT LECs, comparing with the NLO determinations in table 1. Some typical trends of the values of parameters from the NLO study in table 1 to the NNLO one in table 5 are summarized now. The axial-vector decay constant F at leading N_C and chiral limit is reduced at NNLO, which is mainly due to the inclusion of L_4. Our conclusion is based on the fact that strong correlations between F and L_4 always appear, which has been confirmed in previous study [28, 29]. For L_5 and L_8, we find that their values are obviously reduced compared to the NLO determination and become closer to the two-loop results in ref. [27]. As mentioned in the former reference, the discussions in the two-loop SU(3) χPT are sensitive to the value of the $1/N_C$ suppressed LEC L_4. The present study provides an independent determination for this parameter and for the $1/N_C$ suppressed LEC L_6 as well. We mention that our determinations of L_4 have opposite signs with respect to that in ref. [27], which may be the source of the smaller F obtained in that reference. Notice that the present values of L_4, L_5, L_6, L_8 are rather compatible with the combinations of $2L_8 - L_5$ and $2L_6 - L_4$ given in ref. [63]. Fit solutions with larger Λ_1 and Λ_2 than those in eq. (3.4) (out of the a priori range (3.4)) are discarded: they are not considered as reasonable physical solutions and will not be discussed any further. According to the values of α in the two fits, it seems that our study somewhat prefers smaller magnitudes of the $\mathcal{O}(p^6)$ LECs than those from

JHEP06(2015)175

the Dyson-Schwinger approach given in refs. [61, 62] and also prefers a global change of sign with respect to eqs. (3.5) and (3.6). We have investigated the impact of fitting α but releasing one of the $\mathcal{O}(p^6)$ LECs as an independent parameter (e.g., C_{14}), but no definitive conclusion could be extracted. These puzzles cannot be resolved here and it is definitely interesting and necessary to further investigate the values of the $\mathcal{O}(p^6)$ LECs in the future.

The various plots from the NNLO fits are shown in figure 2 for m_η and $m_{\eta'}$, figure 3 for m_K, figure 4 for F_π and F_K, and figure 5 for the ratio F_K/F_π, together with the NLO results and the lattice simulation data and experimental inputs. The shaded area surrounding each curve represents the statistical error band. The figures from NNLOFit-B are compatible with those from NNLOFit-A within the uncertainties, so we only show the results for the former in figures 2, 3, 4 and 5.

In addition, to demonstrate the effects by using the LO masses in the higher order corrections, instead of the renormalized ones, we explicitly show the results for m_η and $m_{\eta'}$ expressed in terms of the LO masses $\overline{m}_\pi, \overline{m}_K$ and $1/F^2$ in figure 2, with the lines labeled as NNLOFit-B-$\overline{m}_{\pi,K}$. The values of the LECs when plotting these lines are exactly the same as those from the NNLOFit-B column in table 5. In this way, one can directly see the differences due to the N^{3}LO truncation uncertainty caused by using the renormalized masses and the LO ones at the NNLO level. According to figure 2, we conclude that the differences for m_η and $m_{\eta'}$ caused by using different types of masses in the higher order corrections are rather within the statistical uncertainties from the fits and therefore the differences should be perfectly compatible within the total uncertainties after taking into account the systematic ones in table 5. We verify that similar conclusions are obtained for other cases. In order not to overload the plots in other figures, we shall not explicitly show the results given in terms of $\overline{m}_\pi$ and $\overline{m}_K$.

From figures 2, 3, 4 and 5, we observe, when compared with the curves of the NLO study, slight improvements in the reproduction of the masses for η, η' and significant ones for m_K, F_π, F_K and the ratios of F_K/F_π. Moreover the χ^2 for the NNLO fits are greatly reduced compared with χ^2 for the NLO ones, indicating that the NNLO corrections are important at the present level of precision and essential to simultaneously describe the lattice simulation data and experimental inputs of the light pseudoscalar mesons π, K, η and η'.

4 Conclusions

In this article we have performed a thorough study on the η-η' mixing, and axial-vector decay constants for the pion and kaon, up to next-to-next-to-leading order in δ expansion within U(3) chiral perturbation theory. We have carried on a detailed scrutiny and discussions of our results, which have been carefully compared to other works in literature for the η-η' mixing. A general mixing formalism, including the higher-derivative terms and kinematic mixing cases, has been addressed in detail. The connections between the mixing parameters from the popular two-mixing-angle scheme and the low energy constants from chiral perturbation theory have been established, both for the singlet-octet basis and the quark-flavor basis.

JHEP06(2015)175

	NNLOFit-A	NNLOFit-B
$\chi^2/(d.o.f)$	212.4/(76-9)	231.9/(76-9)
F (MeV)	81.7±1.5±5.3	80.8±1.6±6.1
$10^3 \times L_5$	0.60±0.11±0.52	0.45±0.12±0.78
$10^3 \times L_8$	0.25±0.07±0.31	0.30±0.06±0.30
Λ_1	-0.003±0.060±0.093	-0.04±0.06±0.13
Λ_2	0.08±0.11±0.20	0.14±0.10±0.40
$10^3 \times L_4$	-0.12±0.06±0.19	-0.09±0.06±0.23
$10^3 \times L_6$	-0.05±0.04±0.02	0.03±0.03±0.02
$10^3 \times L_7$	0.26±0.05±0.06	0.36±0.05±0.12
α	-0.59±0.09±0.18	-0.76±0.08±0.44

Table 5. Parameters from the NNLO fits. In all of these fits, M_0 is fixed at 835.7 MeV from its LO determination. The meaning of different notations to label different fits are explained in detail in the text. The first error bar for each parameter corresponds to the statistical one and the second error denotes the systematic uncertainty. See the text for details.

The considered quantities, including the masses of η, η' and K, the quark mass ratio of $m_s/\widehat{m}$, the parameters in the two-mixing-angle scheme and the π, K decay constants have been confronted with recent lattice simulations and phenomenological inputs. We find that the next-to-leading-order fits yield satisfactory descriptions for the masses of the three pseudoscalar mesons as functions of m_π^2 and the four mixing parameters $(F_0, F_8, \theta_0, \theta_8)$, producing in addition reasonable values of low energy constants. Nonetheless, when the π and K decay constants are included together with the masses and mixing parameters in the fits, the next-to-leading-order analyses are inadequate and it is necessary to step into the next-to-next-to-leading-order study. Using the $\mathcal{O}(p^6)$ LECs determinations from a Dyson-Schwinger-like approach [61, 62] multiplied by a global factor, we are able to achieve a reasonable description for all of the physical quantities considered above and the resulting values for the leading N_C $\mathcal{O}(p^4)$ low energy constants L_5 and L_8 turn to be compatible with the very recent two-loop determinations in ref. [27]. Therefore we conclude that the large N_C U(3) chiral perturbation theory offers a concise theoretical framework that is able to simultaneously reproduce accurately the general η-η' mixing and to provide sophisticated enough expressions to describe the chiral extrapolations of the π and K decay constants and masses.

Our results are also useful for future phenomenological studies of different processes involving η and η'. Combining eq. (2.21) or eq. (2.23) with table 6, one can directly find the relations between the physical states η, η' and the octet-singlet bases η_8, η_0 or the quark-flavor bases η_q, η_s. These relations are consistent with the requirements from the recent lattice simulations and phenomenology.

Finally, it is worthy to remark that some of the parameters in our best analysis (NNLOFit-B) in table 5 have been determined with relatively small errors. For instance,

JHEP06(2015)175

Parameters	Inputs	NNLOFit-A	NNLOFit-B
F_0 (MeV)	118.0 ±16.5	108.0±1.5±3.6	109.1±1.3±5.9
F_8 (MeV)	133.7 ±11.1	124.7±1.2±8.7	126.5±1.2±11.8
θ_0 (Degree)	-11.0 ±3.0	-6.8±1.1±2.6	-6.8±0.9±3.7
θ_8 (Degree)	-26.7 ±5.4	-26.8±1.1±0.2	-27.9±1.0±1.4
$m_s/\widehat{m}$	27.5 ±3.0	27.0±0.6±0.4	29.4±0.4±0.6
F_q (MeV)	106.0 ± 11.1*	92.8±1.1±1.2	92.7±1.0±1.0
F_s (MeV)	143.8 ± 16.5*	136.4±1.5±10.0	139.0±1.4±14.9
θ_q (Degree)	34.5 ± 5.4*	36.4±1.4±0.2	35.8±1.2±0.3
θ_s (Degree)	36.0 ± 4.2*	37.8±0.9±1.5	37.1±0.8±1.1

Table 6. The outputs from NNLO fits. See table 2 for the explanation of the phenomenological inputs. The first error for each quantity corresponds to the statistical one and the second error denotes the systematic one. See the text for details.

the NLO parameters $\Lambda_{1,2}$, which are fitted up to $\mathcal{O}(N_C^{-2})$ in the NNLO analysis, become

$$\Lambda_1 = -0.04 \pm 0.06 \pm 0.13\,, \qquad \Lambda_2 = 0.14 \pm 0.10 \pm 0.40\,. \tag{4.1}$$

The NNLO fit also determines some U(3) NNLO couplings with relatively high precision. NNLOFit-B yields

$$\begin{aligned} &10^3 \times L_4 = -0.09 \pm 0.06 \pm 0.23\,, \qquad 10^3 \times L_6 = 0.03 \pm 0.03 \pm 0.02\,, \\ &10^3 \times L_7 = 0.36 \pm 0.05 \pm 0.12\,. \end{aligned} \tag{4.2}$$

Even though the error estimates in the present article must be considered with some caution, as some lattice systematic uncertainties escape our control, this hints the potentiality of this U(3) χPT framework. We hope these results may encourage future lattice analyses along this line.

Acknowledgments

We thank Shao-Zhou Jiang for communication on the updated values of the $\mathcal{O}(p^6)$ LECs. This work is supported in part by the National Natural Science Foundation of China (NSFC) under Grant No. 11105038, the Natural Science Foundation of Hebei Province with contract No. A2015205205, the grants from the Education Department of Hebei Province under contract No. YQ2014034, the grants from the Department of Human Resources and Social Security of Hebei Province with contract No. C201400323, and the Doctor Foundation of Hebei Normal University under Contract No. L2010B04, the Spanish Government (MINECO) and the European Commission (ERDF) [FPA2010-17747, FPA2013-44773-P, FPA2013-40483-P, SEV-2012-0249 (Severo Ochoa Program), CSD2007-00042 (Consolider Project CPAN)], the grants with contract No. FIS2014-57026-REDT from MINECO (Spain), and EPOS network of the European Community Research Infrastructure Integrating Activity "Study of Strongly Interacting Matter" (HadronPhysics3, Grant No. 283286). J.J. Sanz-Cillero wants to thank the Center for Future High Energy Physics and the Institute of High Energy Physics in Beijing for their hospitality.

JHEP06(2015)175

A Higher order corrections to the $\overline{\eta}$ and $\overline{\eta}'$ bilinear terms

In the following we provide the explicit expressions of the δ_i's in eq. (2.11). When expressing the results in terms of F, they take the form

$$\delta_1 = \frac{32C_{12}}{3F^2}\left[c_\theta^2(4m_K^2 - m_\pi^2) + 4\sqrt{2}c_\theta s_\theta(m_K^2 - m_\pi^2) + s_\theta^2(2m_K^2 + m_\pi^2)\right], \tag{A.1}$$

$$\delta_2 = \frac{32C_{12}}{3F^2}\left[c_\theta^2(2m_K^2 + m_\pi^2) - 4\sqrt{2}c_\theta s_\theta(m_K^2 - m_\pi^2) + s_\theta^2(4m_K^2 - m_\pi^2)\right], \tag{A.2}$$

$$\delta_3 = -\frac{64C_{12}}{3F^2}(m_K^2 - m_\pi^2)\left(\sqrt{2}c_\theta^2 - c_\theta s_\theta - \sqrt{2}s_\theta^2\right), \tag{A.3}$$

$$\begin{aligned}\delta_{\overline{\eta}} = {} & \frac{8L_5[c_\theta^2(4m_K^2 - m_\pi^2) + 4\sqrt{2}c_\theta(m_K^2 - m_\pi^2)s_\theta + (2m_K^2 + m_\pi^2)s_\theta^2]}{3F^2} + s_\theta^2\Lambda_1 \\ & + \frac{c_\theta^2 A_0(m_K^2)}{16\pi^2F^2} + \frac{8L_4(2m_K^2 + m_\pi^2)}{F^2} + \frac{8L_{18}s_\theta[2\sqrt{2}c_\theta(m_K^2 - m_\pi^2) + (2m_K^2 + m_\pi^2)s_\theta]}{F^2} \\ & + \frac{64L_5(L_5 - 2L_8)[c_\theta^2(4m_K^4 - m_\pi^4) + 4\sqrt{2}c_\theta(m_K^4 - m_\pi^4)s_\theta + (2m_K^4 + m_\pi^4)s_\theta^2]}{3F^4} \\ & + \frac{16(C_{14} + C_{17})}{3F^2}[c_\theta^2(8m_K^4 - 8m_K^2m_\pi^2 + 3m_\pi^4) + 8\sqrt{2}c_\theta m_K^2(m_K^2 - m_\pi^2)s_\theta \\ & + (4m_K^4 - 4m_K^2m_\pi^2 + 3m_\pi^4)s_\theta^2],\end{aligned} \tag{A.4}$$

$$\begin{aligned}\delta_{\overline{\eta}'} = {} & \frac{8L_5[c_\theta^2(2m_K^2 + m_\pi^2) + 4\sqrt{2}c_\theta(-m_K^2 + m_\pi^2)s_\theta + (4m_K^2 - m_\pi^2)s_\theta^2]}{3F^2} + c_\theta^2\Lambda_1 \\ & + \frac{s_\theta^2 A_0(m_K^2)}{16\pi^2F^2} + \frac{8L_4(2m_K^2 + m_\pi^2)}{F^2} + \frac{8L_{18}c_\theta[c_\theta(2m_K^2 + m_\pi^2) + 2\sqrt{2}(-m_K^2 + m_\pi^2)s_\theta]}{F^2} \\ & + \frac{64L_5(L_5 - 2L_8)[c_\theta^2(2m_K^4 + m_\pi^4) + 4\sqrt{2}c_\theta(-m_K^4 + m_\pi^4)s_\theta + (4m_K^4 - m_\pi^4)s_\theta^2]}{3F^4} \\ & + \frac{16(C_{14} + C_{17})}{3F^2}[c_\theta^2(4m_K^4 - 4m_K^2m_\pi^2 + 3m_\pi^4) + 8\sqrt{2}c_\theta m_K^2(-m_K^2 + m_\pi^2)s_\theta \\ & + (8m_K^4 - 8m_K^2m_\pi^2 + 3m_\pi^4)s_\theta^2],\end{aligned} \tag{A.5}$$

$$\begin{aligned}\delta_k = {} & -\frac{16L_5(m_K^2 - m_\pi^2)(\sqrt{2}c_\theta^2 - c_\theta s_\theta - \sqrt{2}s_\theta^2)}{3F^2} - c_\theta s_\theta\Lambda_1 \\ & + \frac{c_\theta s_\theta A_0(m_K^2)}{16\pi^2F^2} - \frac{8L_{18}[\sqrt{2}c_\theta^2(m_K^2 - m_\pi^2) + c_\theta(2m_K^2 + m_\pi^2)s_\theta + \sqrt{2}(-m_K^2 + m_\pi^2)s_\theta^2]}{F^2} \\ & - \frac{128L_5(L_5 - 2L_8)(m_K^4 - m_\pi^4)(\sqrt{2}c_\theta^2 - c_\theta s_\theta - \sqrt{2}s_\theta^2)}{3F^4} \\ & - \frac{64(C_{14} + C_{17})m_K^2(m_K^2 - m_\pi^2)(\sqrt{2}c_\theta^2 - c_\theta s_\theta - \sqrt{2}s_\theta^2)}{3F^2},\end{aligned} \tag{A.6}$$

$$\begin{aligned}\delta_{m_{\overline{\eta}}^2} = {} & \frac{16L_8}{3F^2}[c_\theta^2(8m_K^4 - 8m_K^2m_\pi^2 + 3m_\pi^4) + 8\sqrt{2}c_\theta m_K^2(m_K^2 - m_\pi^2)s_\theta \\ & + (4m_K^4 - 4m_K^2m_\pi^2 + 3m_\pi^4)s_\theta^2] \\ & + \frac{2}{3}s_\theta[2\sqrt{2}c_\theta(m_K^2 - m_\pi^2) + (2m_K^2 + m_\pi^2)s_\theta]\Lambda_2\end{aligned}$$

JHEP06(2015)175

$$
\begin{aligned}
&+\frac{1}{16\pi^2}\Bigg\{\frac{1}{18F^2}\Big[c_\theta^4(16m_K^2-7m_\pi^2)+4\sqrt{2}c_\theta^3(8m_K^2-5m_\pi^2)s_\theta+12c_\theta^2(4m_K^2-m_\pi^2)s_\theta^2\\
&+16\sqrt{2}c_\theta(m_K^2-m_\pi^2)s_\theta^3+2(2m_K^2+m_\pi^2)s_\theta^4\Big]A_0(m_\eta^2)\\
&+\frac{(4m_K^2-m_\pi^2)(2c_\theta^4-2\sqrt{2}c_\theta^3s_\theta-3c_\theta^2s_\theta^2+2\sqrt{2}c_\theta s_\theta^3+2s_\theta^4)}{18F^2}A_0(m_{\eta'}^2)\\
&-\frac{[c_\theta^2m_\pi^2+2\sqrt{2}c_\theta(-2m_K^2+m_\pi^2)s_\theta-4m_K^2s_\theta^2]}{3F^2}A_0(m_K^2)\\
&+\frac{m_\pi^2(c_\theta^2-2\sqrt{2}c_\theta s_\theta+2s_\theta^2)}{2F^2}A_0(m_\pi^2)\Bigg\}\\
&-\frac{16L_{25}s_\theta[4\sqrt{2}c_\theta m_K^2(m_K^2-m_\pi^2)+(4m_K^4-4m_K^2m_\pi^2+3m_\pi^4)s_\theta]}{F^2}+6(2m_K^2+m_\pi^2)s_\theta^2v_2^{(2)}\\
&+\frac{16L_6(2m_K^2+m_\pi^2)[c_\theta^2(4m_K^2-m_\pi^2)+4\sqrt{2}c_\theta(m_K^2-m_\pi^2)s_\theta+(2m_K^2+m_\pi^2)s_\theta^2]}{3F^2}\\
&+\frac{16L_7[8c_\theta^2(m_K^2-m_\pi^2)^2+4\sqrt{2}c_\theta(2m_K^4-m_K^2m_\pi^2-m_\pi^4)s_\theta+(2m_K^2+m_\pi^2)^2s_\theta^2]}{3F^2}\\
&+\frac{256(L_5-2L_8)L_8}{3F^4}\Big[c_\theta^2(8m_K^6-4m_K^4m_\pi^2-4m_K^2m_\pi^4+3m_\pi^6)\\
&+4\sqrt{2}c_\theta m_K^2(2m_K^4-m_K^2m_\pi^2-m_\pi^4)s_\theta+(4m_K^6-2m_K^4m_\pi^2-2m_K^2m_\pi^4+3m_\pi^6)s_\theta^2\Big]\\
&+\frac{16(L_5-2L_8)\Lambda_2s_\theta[2\sqrt{2}c_\theta(m_K^4-m_\pi^4)+(2m_K^4+m_\pi^4)s_\theta]}{3F^2}\\
&+\frac{16(3C_{19}+2C_{31})}{3F^2}\Big[c_\theta^2(16m_K^6-24m_K^4m_\pi^2+12m_K^2m_\pi^4-m_\pi^6)\\
&+4\sqrt{2}c_\theta(4m_K^6-6m_K^4m_\pi^2+3m_K^2m_\pi^4-m_\pi^6)s_\theta\\
&+(8m_K^6-12m_K^4m_\pi^2+6m_K^2m_\pi^4+m_\pi^6)s_\theta^2\Big],
\end{aligned}
\tag{A.7}
$$

$$
\begin{aligned}
\delta_{m_{\bar\eta}^2}=\;&\frac{2}{3}c_\theta[c_\theta(2m_K^2+m_\pi^2)+2\sqrt{2}(-m_K^2+m_\pi^2)s_\theta]\Lambda_2\\
&+\frac{16L_8}{3F^2}[c_\theta^2(4m_K^4-4m_K^2m_\pi^2+3m_\pi^4)+8\sqrt{2}c_\theta m_K^2(-m_K^2+m_\pi^2)s_\theta\\
&+(8m_K^4-8m_K^2m_\pi^2+3m_\pi^4)s_\theta^2]\\
&+\frac{1}{16\pi^2}\Bigg\{\frac{(4m_K^2-m_\pi^2)(2c_\theta^4-2\sqrt{2}c_\theta^3s_\theta-3c_\theta^2s_\theta^2+2\sqrt{2}c_\theta s_\theta^3+2s_\theta^4)}{18F^2}A_0(m_\eta^2)\\
&+\frac{1}{18F^2}\Big[2c_\theta^4(2m_K^2+m_\pi^2)-16\sqrt{2}c_\theta^3(m_K^2-m_\pi^2)s_\theta+12c_\theta^2(4m_K^2-m_\pi^2)s_\theta^2\\
&-4\sqrt{2}c_\theta(8m_K^2-5m_\pi^2)s_\theta^3+(16m_K^2-7m_\pi^2)s_\theta^4\Big]A_0(m_{\eta'}^2)\\
&-\frac{[-4c_\theta^2m_K^2+2\sqrt{2}c_\theta(2m_K^2-m_\pi^2)s_\theta+m_\pi^2s_\theta^2]}{3F^2}A_0(m_K^2)\\
&+\frac{m_\pi^2(2c_\theta^2+2\sqrt{2}c_\theta s_\theta+s_\theta^2)}{2F^2}A_0(m_\pi^2)\Bigg\}\\
&-\frac{16L_{25}c_\theta[c_\theta(4m_K^4-4m_K^2m_\pi^2+3m_\pi^4)+4\sqrt{2}m_K^2(-m_K^2+m_\pi^2)s_\theta]}{F^2}
\end{aligned}
$$

JHEP06(2015)175

$$
\begin{aligned}
&+6c_\theta^2(2m_K^2+m_\pi^2)v_2^{(2)}\\
&+\frac{16L_7[c_\theta^2(2m_K^2+m_\pi^2)^2+4\sqrt{2}c_\theta(-2m_K^4+m_K^2m_\pi^2+m_\pi^4)s_\theta+8(m_K^2-m_\pi^2)^2s_\theta^2]}{3F^2}\\
&+\frac{16L_6(2m_K^2+m_\pi^2)[c_\theta^2(2m_K^2+m_\pi^2)+4\sqrt{2}c_\theta(-m_K^2+m_\pi^2)s_\theta+(4m_K^2-m_\pi^2)s_\theta^2]}{3F^2}\\
&+\frac{256(L_5-2L_8)L_8}{3F^4}[c_\theta^2(4m_K^6-2m_K^4m_\pi^2-2m_K^2m_\pi^4+3m_\pi^6)+\\
&4\sqrt{2}c_\theta m_K^2(-2m_K^4+m_K^2m_\pi^2+m_\pi^4)s_\theta+(8m_K^6-4m_K^4m_\pi^2-4m_K^2m_\pi^4+3m_\pi^6)s_\theta^2]\\
&+\frac{16(L_5-2L_8)\Lambda_2c_\theta[2\sqrt{2}s_\theta(-m_K^4+m_\pi^4)+(2m_K^4+m_\pi^4)c_\theta]}{3F^2}\\
&+\frac{16(3C_{19}+2C_{31})}{3F^2}\Big[c_\theta^2(8m_K^6-12m_K^4m_\pi^2+6m_K^2m_\pi^4+m_\pi^6)\\
&-4\sqrt{2}c_\theta(4m_K^6-6m_K^4m_\pi^2+3m_K^2m_\pi^4-m_\pi^6)s_\theta\\
&+(16m_K^6-24m_K^4m_\pi^2+12m_K^2m_\pi^4-m_\pi^6)s_\theta^2\Big],
\end{aligned}
\tag{A.8}
$$

$$
\begin{aligned}
\delta_{m^2}=&-\frac{64L_8m_K^2(m_K^2-m_\pi^2)(\sqrt{2}c_\theta^2-c_\theta s_\theta-\sqrt{2}s_\theta^2)}{3F^2}\\
&-\frac{2}{3}[\sqrt{2}c_\theta^2(m_K^2-m_\pi^2)+c_\theta(2m_K^2+m_\pi^2)s_\theta+\sqrt{2}(-m_K^2+m_\pi^2)s_\theta^2]\Lambda_2\\
&-\frac{1}{288\pi^2F^2}\Big\{\Big[\sqrt{2}c_\theta^4(8m_K^2-5m_\pi^2)+c_\theta^3(8m_K^2+m_\pi^2)s_\theta+3\sqrt{2}c_\theta^2(-4m_K^2+m_\pi^2)s_\theta^2\\
&+4c_\theta(-5m_K^2+2m_\pi^2)s_\theta^3+4\sqrt{2}(-m_K^2+m_\pi^2)s_\theta^4\Big]A_0(m_\eta^2)\\
&+\Big[4\sqrt{2}c_\theta^4(m_K^2-m_\pi^2)+3\sqrt{2}c_\theta^2(4m_K^2-m_\pi^2)s_\theta^2+c_\theta(8m_K^2+m_\pi^2)s_\theta^3\\
&+\sqrt{2}(-8m_K^2+5m_\pi^2)s_\theta^4+4c_\theta^3s_\theta(-5m_K^2+2m_\pi^2)\Big]A_0(m_{\eta'}^2)\\
&+6[\sqrt{2}c_\theta^2(2m_K^2-m_\pi^2)+c_\theta(4m_K^2+m_\pi^2)s_\theta+\sqrt{2}(-2m_K^2+m_\pi^2)s_\theta^2]A_0(m_K^2)\\
&+9m_\pi^2(-\sqrt{2}c_\theta^2+c_\theta s_\theta+\sqrt{2}s_\theta^2)A_0(m_\pi^2)\Big\}\\
&-6c_\theta(2m_K^2+m_\pi^2)s_\theta v_2^{(2)}-\frac{32L_6(2m_K^4-m_K^2m_\pi^2-m_\pi^4)(\sqrt{2}c_\theta^2-c_\theta s_\theta-\sqrt{2}s_\theta^2)}{3F^2}\\
&+\frac{16L_{25}}{F^2}\Big[2\sqrt{2}c_\theta^2m_K^2(m_K^2-m_\pi^2)+c_\theta(4m_K^4-4m_K^2m_\pi^2+3m_\pi^4)s_\theta\\
&+2\sqrt{2}m_K^2(-m_K^2+m_\pi^2)s_\theta^2\Big]\\
&-\frac{16L_7}{3F^2}\Big[2\sqrt{2}c_\theta^2(2m_K^4-m_K^2m_\pi^2-m_\pi^4)+c_\theta(-4m_K^4+20m_K^2m_\pi^2-7m_\pi^4)s_\theta+\\
&2\sqrt{2}(-2m_K^4+m_K^2m_\pi^2+m_\pi^4)s_\theta^2\Big]\\
&-\frac{512(L_5-2L_8)L_8m_K^2(2m_K^4-m_K^2m_\pi^2-m_\pi^4)(\sqrt{2}c_\theta^2-c_\theta s_\theta-\sqrt{2}s_\theta^2)}{3F^4}\\
&-\frac{16(L_5-2L_8)\Lambda_2[\sqrt{2}c_\theta^2(m_K^4-m_\pi^4)+c_\theta(2m_K^4+m_\pi^4)s_\theta+\sqrt{2}(-m_K^4+m_\pi^4)s_\theta^2]}{3F^2}\\
&-\frac{32(3C_{19}+2C_{31})(4m_K^6-6m_K^4m_\pi^2+3m_K^2m_\pi^4-m_\pi^6)(\sqrt{2}c_\theta^2-c_\theta s_\theta-\sqrt{2}s_\theta^2)}{3F^2}.
\end{aligned}
\tag{A.9}
$$

JHEP06(2015)175

When expressing the above results in terms of F_π from eq. (2.27), the terms with L_5^2 and L_5L_8 can be different from the expressions in terms of F and the other parts remain the same, apart from the obvious replacement of F by F_π. Therefore, for the expressions of δ_i expressed in F_π, we only give the parts that are different from those in terms of F

$$\delta_{\overline{\eta}}^{(F_\pi),L_5^2} = \frac{128L_5^2}{3F_\pi^4}\Big[c_\theta^2(2m_K^4+2m_K^2m_\pi^2-m_\pi^4)+2\sqrt{2}c_\theta s_\theta(m_K^4+m_K^2m_\pi^2-2m_\pi^4) +s_\theta^2(m_K^4+m_K^2m_\pi^2+m_\pi^4)\Big], \tag{A.10}$$

$$\delta_{\overline{\eta}'}^{(F_\pi),L_5^2} = \frac{128L_5^2}{3F_\pi^4}\Big[c_\theta^2(m_K^4+m_K^2m_\pi^2+m_\pi^4)-2\sqrt{2}c_\theta s_\theta(m_K^4+m_K^2m_\pi^2-2m_\pi^4) +s_\theta^2(2m_K^4+2m_K^2m_\pi^2-m_\pi^4)\Big], \tag{A.11}$$

$$\delta_k^{(F_\pi),L_5^2} = -\frac{128L_5^2(m_K^4+m_K^2m_\pi^2-2m_\pi^4)(\sqrt{2}c_\theta^2-c_\theta s_\theta-\sqrt{2}s_\theta^2)}{3F_\pi^4}, \tag{A.12}$$

$$\delta_{m_{\overline{\eta}}^2}^{(F_\pi),L_5L_8} = \frac{128L_5L_8}{3F_\pi^4}\Big[c_\theta^2(16m_K^6-16m_K^2m_\pi^4+9m_\pi^6)+16\sqrt{2}c_\theta m_K^2(m_K^4-m_\pi^4)s_\theta +(8m_K^6-8m_K^2m_\pi^4+9m_\pi^6)s_\theta^2\Big], \tag{A.13}$$

$$\delta_{m_{\overline{\eta}'}^2}^{(F_\pi),L_5L_8} = \frac{128L_5L_8}{3F_\pi^4}\Big[c_\theta^2(8m_K^6-8m_K^2m_\pi^4+9m_\pi^6)-16\sqrt{2}c_\theta m_K^2(m_K^4-m_\pi^4)s_\theta +(16m_K^6-16m_K^2m_\pi^4+9m_\pi^6)s_\theta^2\Big], \tag{A.14}$$

$$\delta_{m^2}^{(F_\pi),L_5L_8} = -\frac{1024L_5L_8m_K^2(m_K^4-m_\pi^4)(\sqrt{2}c_\theta^2-c_\theta s_\theta-\sqrt{2}s_\theta^2)}{3F_\pi^4}. \tag{A.15}$$

In order to obtain the full expressions for the δ_i's given in terms of F_π one has to make use of eq. (2.27) up to the precision required. Taking δ_k for example, its final expression in terms of F_π is

$$\begin{aligned}\delta_k = &-\frac{16L_5(m_K^2-m_\pi^2)(\sqrt{2}c_\theta^2-c_\theta s_\theta-\sqrt{2}s_\theta^2)}{3F_\pi^2}-c_\theta s_\theta\Lambda_1\\ &+\frac{c_\theta s_\theta A_0(m_K^2)}{16\pi^2F_\pi^2}-\frac{8L_{18}[\sqrt{2}c_\theta^2(m_K^2-m_\pi^2)+c_\theta(2m_K^2+m_\pi^2)s_\theta+\sqrt{2}(-m_K^2+m_\pi^2)s_\theta^2]}{F_\pi^2}\\ &+\frac{256L_5L_8(m_K^4-m_\pi^4)(\sqrt{2}c_\theta^2-c_\theta s_\theta-\sqrt{2}s_\theta^2)}{3F_\pi^4}\\ &-\frac{128L_5^2(m_K^4+m_K^2m_\pi^2-2m_\pi^4)(\sqrt{2}c_\theta^2-c_\theta s_\theta-\sqrt{2}s_\theta^2)}{3F_\pi^4}\\ &-\frac{64(C_{14}+C_{17})m_K^2(m_K^2-m_\pi^2)(\sqrt{2}c_\theta^2-c_\theta s_\theta-\sqrt{2}s_\theta^2)}{3F_\pi^2},\end{aligned} \tag{A.16}$$

which differs from eq. (A.6) in the L_5^2 term. For δ_1, δ_2 and δ_3, their expressions are the same regardless of whether F or F_π is chosen up to next-to-next-to-leading order.

For completeness, we also give the results in terms of the LO masses $\overline{m}_\pi$ and $\overline{m}_K$ and $1/F^2$. Only the terms with L_iL_j, being L_i and L_j the NLO LECs in eq. (2.4), will be different, comparing with the expressions in terms of m_π and m_K and the other parts

JHEP06(2015)175

remain the same, apart from the obvious replacement of the renormalized masses by the LO ones. Therefore, we only give the parts that are different from those in terms of m_π, m_K and $1/F^2$ and it turns out that in this case all of the L_iL_j terms for $\delta_{\overline{\eta}}, \delta_{\overline{\eta}'}, \delta_k, \delta_{m^2_{\overline{\eta}}}, \delta_{m^2_{\overline{\eta}'}}, \delta_{m^2}$ vanish.

Open Access. This article is distributed under the terms of the Creative Commons Attribution License (CC-BY 4.0), which permits any use, distribution and reproduction in any medium, provided the original author(s) and source are credited.

References

[1] J. Gasser and H. Leutwyler, *Chiral Perturbation Theory to One Loop*, *Annals Phys.* **158** (1984) 142 [INSPIRE].

[2] J. Gasser and H. Leutwyler, *Chiral Perturbation Theory: Expansions in the Mass of the Strange Quark*, *Nucl. Phys.* **B 250** (1985) 465 [INSPIRE].

[3] G. 't Hooft, *A Planar Diagram Theory for Strong Interactions*, *Nucl. Phys.* **B 72** (1974) 461 [INSPIRE].

[4] G. 't Hooft, *A Two-Dimensional Model for Mesons*, *Nucl. Phys.* **B 75** (1974) 461.

[5] E. Witten, *Baryons in the 1/n Expansion*, *Nucl. Phys.* **B 160** (1979) 57 [INSPIRE].

[6] P. Di Vecchia and G. Veneziano, *Chiral Dynamics in the Large-N Limit*, *Nucl. Phys.* **B 171** (1980) 253 [INSPIRE].

[7] C. Rosenzweig, J. Schechter and C.G. Trahern, *Is the Effective Lagrangian for QCD a σ-model?*, *Phys. Rev.* **D 21** (1980) 3388 [INSPIRE].

[8] E. Witten, *Large-N Chiral Dynamics*, *Annals Phys.* **128** (1980) 363 [INSPIRE].

[9] K. Kawarabayashi and N. Ohta, *The Problem of η in the Large-N Limit: Effective Lagrangian Approach*, *Nucl. Phys.* **B 175** (1980) 477 [INSPIRE].

[10] H. Leutwyler, *On the 1/N expansion in chiral perturbation theory*, *Nucl. Phys. Proc. Suppl.* **64** (1998) 223 [hep-ph/9709408] [INSPIRE].

[11] R. Kaiser and H. Leutwyler, *Pseudoscalar decay constants at large-N_c*, hep-ph/9806336 [INSPIRE].

[12] R. Kaiser and H. Leutwyler, *Large-N_c in chiral perturbation theory*, *Eur. Phys. J.* **C 17** (2000) 623 [hep-ph/0007101] [INSPIRE].

[13] P. Herrera-Siklody, J.I. Latorre, P. Pascual and J. Taron, *Chiral effective Lagrangian in the large-N_c limit: The Nonet case*, *Nucl. Phys.* **B 497** (1997) 345 [hep-ph/9610549] [INSPIRE].

[14] P. Herrera-Siklody, J.I. Latorre, P. Pascual and J. Taron, *Eta - eta-prime mixing from U(3)(L) $\times$ U(3)(R) chiral perturbation theory*, *Phys. Lett.* **B 419** (1998) 326 [hep-ph/9710268] [INSPIRE].

[15] J.J. Dudek et al., *Isoscalar meson spectroscopy from lattice QCD*, *Phys. Rev.* **D 83** (2011) 111502 [arXiv:1102.4299] [INSPIRE].

[16] N.H. Christ et al., *The η and η' mesons from Lattice QCD*, *Phys. Rev. Lett.* **105** (2010) 241601 [arXiv:1002.2999] [INSPIRE].

JHEP06(2015)175

[17] UKQCD collaboration, E.B. Gregory, A.C. Irving, C.M. Richards and C. McNeile, *A study of the eta and eta' mesons with improved staggered fermions*, *Phys. Rev.* **D 86** (2012) 014504 [arXiv:1112.4384] [INSPIRE].

[18] EUROPEAN TWISTED MASS collaboration, C. Michael et al., *η and η' masses and decay constants from lattice QCD with $N_f = 2 + 1 + 1$ quark flavours*, PoS(LATTICE 2013)253 [arXiv:1311.5490].

[19] ETM collaboration, C. Michael, K. Ottnad and C. Urbach, *η and η' mixing from Lattice QCD*, *Phys. Rev. Lett.* **111** (2013) 181602 [arXiv:1310.1207] [INSPIRE].

[20] Y.-H. Chen, Z.-H. Guo and H.-Q. Zheng, *Study of η-η' mixing from radiative decay processes*, *Phys. Rev.* **D 85** (2012) 054018 [arXiv:1201.2135] [INSPIRE].

[21] Y.-H. Chen, Z.-H. Guo and B.-S. Zou, *Unified study of $J/\psi \to PV$, $P\gamma^{(*)}$ and light hadron radiative processes*, *Phys. Rev.* **D 91** (2015) 014010 [arXiv:1411.1159] [INSPIRE].

[22] RBC, UKQCD collaboration, Y. Aoki et al., *Continuum Limit Physics from 2+1 Flavor Domain Wall QCD*, *Phys. Rev.* **D 83** (2011) 074508 [arXiv:1011.0892] [INSPIRE].

[23] RBC and UKQCD collaborations, R. Arthur et al., *Domain Wall QCD with Near-Physical Pions*, *Phys. Rev.* **D 87** (2013) 094514 [arXiv:1208.4412] [INSPIRE].

[24] S. Dürr et al., *The ratio FK/Fpi in QCD*, *Phys. Rev.* **D 81** (2010) 054507 [arXiv:1001.4692] [INSPIRE].

[25] S. Descotes-Genon, L. Girlanda and J. Stern, *Paramagnetic effect of light quark loops on chiral symmetry breaking*, *JHEP* **01** (2000) 041 [hep-ph/9910537] [INSPIRE].

[26] J. Bijnens and I. Jemos, *A new global fit of the L_i^r at next-to-next-to-leading order in Chiral Perturbation Theory*, *Nucl. Phys.* **B 854** (2012) 631 [arXiv:1103.5945] [INSPIRE].

[27] J. Bijnens and G. Ecker, *Mesonic low-energy constants*, *Ann. Rev. Nucl. Part. Sci.* **64** (2014) 149 [arXiv:1405.6488] [INSPIRE].

[28] G. Ecker, P. Masjuan and H. Neufeld, *Approximating chiral* SU(3) *amplitudes*, *Eur. Phys. J.* **C 74** (2014) 2748 [arXiv:1310.8452] [INSPIRE].

[29] Z.-H. Guo and J.J. Sanz-Cillero, *Resonance effects in pion and kaon decay constants*, *Phys. Rev.* **D 89** (2014) 094024 [arXiv:1403.0855] [INSPIRE].

[30] T. Feldmann, P. Kroll and B. Stech, *Mixing and decay constants of pseudoscalar mesons*, *Phys. Rev.* **D 58** (1998) 114006 [hep-ph/9802409] [INSPIRE].

[31] R. Escribano and J.-M. Frere, *Study of the η-η' system in the two mixing angle scheme*, *JHEP* **06** (2005) 029 [hep-ph/0501072] [INSPIRE].

[32] C.E. Thomas, *Composition of the Pseudoscalar η and η' Mesons*, *JHEP* **10** (2007) 026 [arXiv:0705.1500] [INSPIRE].

[33] G. Li, Q. Zhao and C.-H. Chang, *Decays of J/ψ and ψ' into vector and pseudoscalar meson and the pseudoscalar glueball-$q\bar{q}$ mixing*, *J. Phys.* **G 35** (2008) 055002 [hep-ph/0701020] [INSPIRE].

[34] R. Escribano, P. Masjuan and P. Sanchez-Puertas, *η and η' transition form factors from rational approximants*, *Phys. Rev.* **D 89** (2014) 034014 [arXiv:1307.2061] [INSPIRE].

[35] F. De Fazio and M.R. Pennington, *Radiative phi meson decays and η-η' mixing: A QCD sum rule analysis*, *JHEP* **07** (2000) 051 [hep-ph/0006007] [INSPIRE].

JHEP06(2015)175

[36] J. Schechter, A. Subbaraman and H. Weigel, *Effective hadron dynamics: from meson masses to the proton spin puzzle*, *Phys. Rev.* **D 48** (1993) 339 [hep-ph/9211239] [INSPIRE].

[37] E. Witten, *Current Algebra Theorems for the* U(1) *Goldstone Boson*, *Nucl. Phys.* **B 156** (1979) 269 [INSPIRE].

[38] S.R. Coleman and E. Witten, *Chiral Symmetry Breakdown in Large-N Chromodynamics*, *Phys. Rev. Lett.* **45** (1980) 100 [INSPIRE].

[39] G. Veneziano, U(1) *Without Instantons*, *Nucl. Phys.* **B 159** (1979) 213 [INSPIRE].

[40] S.-Z. Jiang, F.-J. Ge and Q. Wang, *Full pseudoscalar mesonic chiral Lagrangian at p^6 order under the unitary group*, *Phys. Rev.* **D 89** (2014) 074048 [arXiv:1401.0317] [INSPIRE].

[41] N. Beisert and B. Borasoy, *$\eta\eta'$ mixing in* U(3) *chiral perturbation theory*, *Eur. Phys. J.* **A 11** (2001) 329 [hep-ph/0107175] [INSPIRE].

[42] J.-M. Gerard and E. Kou, *eta-eta-prime masses and mixing: a large-N_c reappraisal*, *Phys. Lett.* **B 616** (2005) 85 [hep-ph/0411292] [INSPIRE].

[43] C. Degrande and J.-M. Gerard, *A Theoretical determination of the η-η' mixing*, *JHEP* **05** (2009) 043 [arXiv:0901.2860] [INSPIRE].

[44] V. Mathieu and V. Vento, *η-η' mixing in the flavor basis and large-N*, *Phys. Lett.* **B 688** (2010) 314 [arXiv:1003.2119] [INSPIRE].

[45] Z.-H. Guo and J.A. Oller, *Resonances from meson-meson scattering in* U(3) *ChPT*, *Phys. Rev.* **D 84** (2011) 034005 [arXiv:1104.2849] [INSPIRE].

[46] J. Bijnens, G. Colangelo and G. Ecker, *The Mesonic chiral Lagrangian of order p^6*, *JHEP* **02** (1999) 020 [hep-ph/9902437] [INSPIRE].

[47] Z.-H. Guo, J.A. Oller and J. Ruiz de Elvira, *Chiral dynamics in form factors, spectral-function sum rules, meson-meson scattering and semi-local duality*, *Phys. Rev.* **D 86** (2012) 054006 [arXiv:1206.4163] [INSPIRE].

[48] G. Amoros, J. Bijnens and P. Talavera, *QCD isospin breaking in meson masses, decay constants and quark mass ratios*, *Nucl. Phys.* **B 602** (2001) 87 [hep-ph/0101127] [INSPIRE].

[49] H. Georgi, *A bound on $m(\eta)/m(\eta')$ for large-N_c*, *Phys. Rev.* **D 49** (1994) 1666 [hep-ph/9310337] [INSPIRE].

[50] S. Peris, *Higher order corrections to the large-N_c bound on $M(\eta)/M(\eta')$*, *Phys. Lett.* **B 324** (1994) 442 [hep-ph/9312239] [INSPIRE].

[51] T. Feldmann, *Quark structure of pseudoscalar mesons*, *Int. J. Mod. Phys.* **A 15** (2000) 159 [hep-ph/9907491] [INSPIRE].

[52] G. Amoros, J. Bijnens and P. Talavera, *Two point functions at two loops in three flavor chiral perturbation theory*, *Nucl. Phys.* **B 568** (2000) 319 [hep-ph/9907264] [INSPIRE].

[53] V. Bernard and E. Passemar, *Chiral Extrapolation of the Strangeness Changing $K\pi$ Form Factor*, *JHEP* **04** (2010) 001 [arXiv:0912.3792] [INSPIRE].

[54] S. Aoki et al., *Review of lattice results concerning low-energy particle physics*, *Eur. Phys. J.* **C 74** (2014) 2890 [arXiv:1310.8555] [INSPIRE].

[55] Particle Data Group collaboration, *Review of Particle Physics*, *Chin. Phys.* **C 38** (2014) 090001 [INSPIRE].

JHEP06(2015)175

[56] R. Escribano, P. Masjuan and J.J. Sanz-Cillero, *Chiral dynamics predictions for $\eta' \to \eta\pi\pi$*, *JHEP* **05** (2011) 094 [arXiv:1011.5884] [INSPIRE].

[57] G. Ecker, J. Gasser, A. Pich and E. de Rafael, *The Role of Resonances in Chiral Perturbation Theory*, *Nucl. Phys.* **B 321** (1989) 311 [INSPIRE].

[58] I. Rosell, J.J. Sanz-Cillero and A. Pich, *Towards a determination of the chiral couplings at NLO in $1/N_C$: $L_8^r(\mu)$*, *JHEP* **01** (2007) 039 [hep-ph/0610290] [INSPIRE].

[59] J.J. Sanz-Cillero and J. Trnka, *High energy constraints in the octet SS-PP correlator and resonance saturation at NLO in $1/N_c$*, *Phys. Rev.* **D 81** (2010) 056005 [arXiv:0912.0495] [INSPIRE].

[60] M. Jamin, J.A. Oller and A. Pich, *S wave K pi scattering in chiral perturbation theory with resonances*, *Nucl. Phys.* **B 587** (2000) 331 [hep-ph/0006045] [INSPIRE].

[61] S.-Z. Jiang, Y. Zhang, C. Li and Q. Wang, *Computation of the p^6 order chiral Lagrangian coefficients*, *Phys. Rev.* **D 81** (2010) 014001 [arXiv:0907.5229] [INSPIRE].

[62] S.-Z. Jiang, Z.-L. Wei, Q.-S. Chen and Q. Wang, *Computation of the $O(p^6)$ order low-energy constants: an update*, arXiv:1502.05087 [INSPIRE].

[63] J.A. Oller and L. Roca, *Non-Perturbative Study of the Light Pseudoscalar Masses in Chiral Dynamics*, *Eur. Phys. J.* **A 34** (2007) 371 [hep-ph/0608290] [INSPIRE].

JHEP06(2015)175